Author(s): Brazeau, Allison; Hänninen, Mikko M.; Tuononen, Heikki; Jones, Nathan; Ragogna, Paul

Title: Synthesis, Reactivity, and Computational Analysis of Halophosphines Supported by Dianionic Guanidinate Ligands

Year: 2012

Version:

Please cite the original version:

Brazeau, A., Hänninen, M. M., Tuononen, H., Jones, N., & Ragogna, P. (2012). Synthesis, Reactivity, and Computational Analysis of Halophosphines Supported by Dianionic Guanidinate Ligands. Journal of the American Chemical Society, 134(11), 5398-5414. https://doi.org/10.1021/ja300587z

Synthesis, reactivity and computational analysis of halophosphines supported by dianionic guanidinate ligands

*Allison L. Brazeau[1], Mikko M. Hänninen[2], Heikki M. Tuononen[2], Nathan D. Jones[1], and Paul J. Ragogna[1]**

[1]Department of Chemistry, The University of Western Ontario, Chemistry Building, 1151 Richmond St., London, Ontario, Canada, N6A 5B7

[2]Department of Chemistry, P.O. Box 35, FI-40014 University of Jyväskylä, Finland

*To whom correspondence should be addressed. Tel: 1-519-661-2111 ext: 87048. Fax: 1-519-661-3022. Email: pragogna@uwo.ca

Abstract

The reported chemistry and reactivity of guanidinate supported group 15 elements in the +3 oxidation state, particularly phosphorus, is limited when compared to their ubiquity in supporting metallic elements across the periodic table. We have synthesized a series of chlorophosphines utilizing homo- and heteroleptic (dianionic)guanidinates and have completed a comprehensive study of their reactivity. Most notable is the reluctancy of these four-membered rings to form the corresponding *N*-heterocyclic phosphenium cations, the tendency to chemically and thermally eliminate carbodiimide and the scarcely observed ring expansion by insertion of a chloro(imino)phosphine into a P–N bond of the P–N–C–N framework. Computational analysis has provided corroborating evidence for the unwillingness of the halide abstraction reaction by demonstrating the exceptional electron acceptor properties of the target phosphenium cations and the underscoring strength of the P–X bond.

Introduction

A major theme in the field of synthetic main group chemistry is to push the limits of the bonding environments surrounding a central p-block element and impose a stress that will then allow for access to unprecedented yet controlled reactivity. There are many variables associated with forcing such a condition within a molecule that include modifications to the electronics, sterics, charge and ring strain. Over the past decade there has been a shift in research efforts to design main group molecules that are capable of reactivity previously reserved for the transition metals. Highlights include the ability of "frustrated Lewis pairs," low-valent group 13 species, and heavy group 14 analogues of *N*-heterocyclic carbenes, alkenes and alkynes to activate small molecules, including H_2, NH_3, PH_3, and P_4.

Power *et al*. were the first to demonstrate the bifurcation of dihydrogen by a main group metal, with the addition of H_2 across the Ge≡Ge bond in unsaturated digermynes at ambient temperature and pressure to give a combination of digermenes and germanes.[1] Several years later he also showed the addition of dihydrogen to distannynes to give tin(II) hydrides.[2-8] A notable surge in the reported

reactivity of "frustrated Lewis pairs" (FLP) was kickstarted by Stephan *et al.,* where they reported metal-free reversible hydrogen activation by the unquenched reactivity of a phosphine-borane ($(C_6H_2Me_3)_2P(C_6F_4)B(C_6F_5)_2$), which features a Lewis acidic boron and Lewis basic phosphorus.[9] Since then, many different FLP systems have been developed[10] and reactivity with a variety of substrates has been observed, including B-H bonds,[11] CO_2,[12,13] unsaturated bonds[10] and even catalytic, metal-free hydrogenation.[14-18]

The silylene LSi (L = CH{(C=CH_2)(CMe)(2,6-^{i}Pr$_2$C$_6$H$_3$N)$_2$}) will oxidatively add ammonia to give four-coordinate LSi(H)NH_2[19] and is the only reported main group molecule that has been successfully used in the activation of PH_3, yielding LSi(H)PH_2.[20]

Phosphenium cations $[R_2P]^+$ are a class of phosphorus-containing molecules that have a rich history of reactivity, including reactions with Lewis bases,[21-23] inorganic and organic unsaturated bonds,[24] and as ligands on transition metals.[25-32] Phosphenium cations are also known to catenate, which is demonstrated by the many examples from Burford *et al*. in which a $[R_2P]^+$ fragment is inserted into cyclic and acyclic P–P bonds, to expand the ring or chain by an additional P atom to give *catena*-polyphosphorus cations.[33] Weigand has recently shown the ability of phosphenium cations to activate small molecules by novel examples of controlled reactivity with P_4 using a *N*-heterocyclic phosphenium cation (NHP) supported within a strained four-membered ring system to form cationic P_5 clusters.[34,35] Substitution reactions on acyclic cations of the type $[LPCl_2]^+$ and $[L_2PCl]^{2+}$ to replace the Cl with CN- or N_3-groups have also been accomplished by this same group.[36]

The phosphenium cation in particular presents a unique environment where the molecule is Lewis amphoteric given that the cationic phosphorus atom can be an electron donor or electron acceptor, which opens the floodgates for unique structures, bonding arrangements and reactivity. The NHP is isovalent with the *N*-heterocyclic carbene (NHC) but has inverse electronic properties, in that they are poor σ-donors but have excellent π-accepting capabilities (Chart 1a).

We envisaged designing a NHP within a highly strained four-membered ring so that the phosphorus atom could be probed for new and unobserved reactivity. While several four-membered

rings incorporating NHP are known (Chart 1b) they are all of the type P–N–X–N where X = P,[34,37] Si or Al,[35,38] all electropositive elements, however the example where X = C has surprisingly been absent from the literature. We sought to extend this series and fill the void by using the nitrogen-based, chelating, guanidinate ligand (Chart 2a,b), which despite its wide spread use for supporting metallic elements spanning the periodic table, little is known about the role in stabilizing group 15 centres in the +3 oxidation state. Jones *et al*. have synthesized several (monoanionic)guanidinate pnictogen(III) dihalides (pnictogen = Pn = P, As, Sb) as precursors to amido-dipnictenes (Chart 3c).[39] Related (monoanionic)amidinate ligands (Chart 2c) have been used in stabilizing heavier group 15 atoms (As, Sb, Bi)[40-43] as shown in Chart 3a,b. We have previously reported a (monoanionic)guanidinate ligand capable of supporting a dicationic arsenic centre with additional stabilization from a Lewis base (Chart 3c).[44] For the synthesis of an NHP it would be ideal to have the "free" cation, which therefore calls for the use of a (dianionic)guanidinate (Chart 2b). There is only one previous report of a (dianionic)guanidinate being used to support a group 15 atom involving antimony[45] (Chart 3d), and one example of a phosphorus centre[39] being supported by a guanidinate ligand.

Chart 1. a) NHC vs. NHP and b) known and target four-membered NHP species.

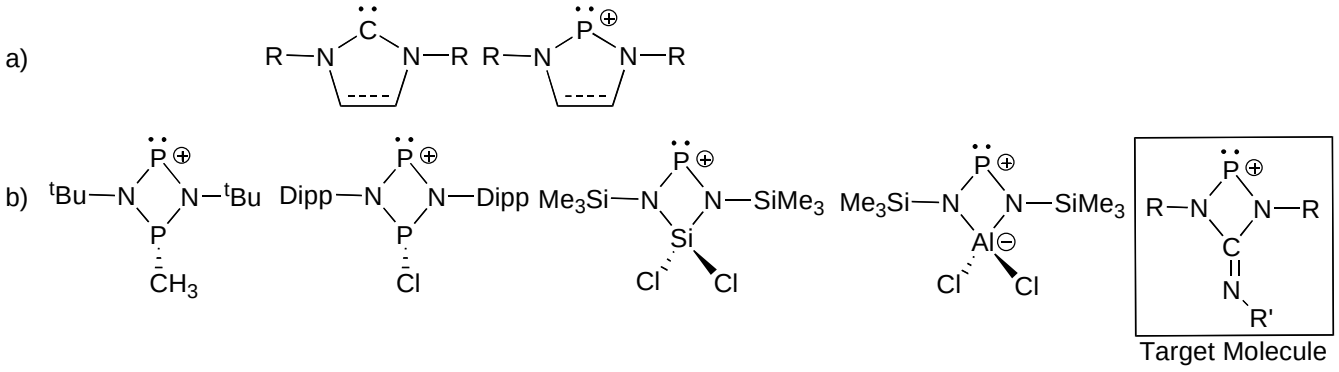

Chart 2. a) Monoanionic vs. b) dianionic guanidinate ligands, and c) amidinate ligands

a) 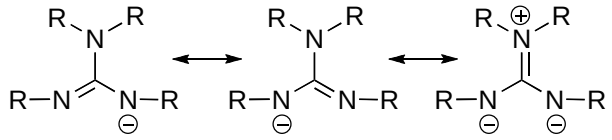

b) 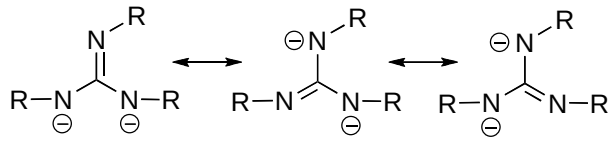

c) 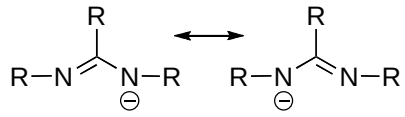

Chart 3. Literature examples of a) monomeric (monoanionic)amidinate, b) dimeric (monoanionic)amidinate, c) (monoanionic)guanidinate, and d) (dianionic)guanidinate ligands.

a)

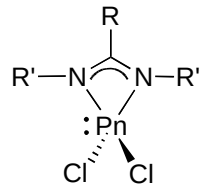

Pn = As, R = ^{t}Bu, R' = Dipp
Pn = Sb, R = ^{t}Bu, R' = Cy
Pn = Sb, R = ^{t}Bu, R' = ^{i}Pr
Pn = Sb, R = ^{t}Bu, R' = Dipp
Pn = Sb, R = ^{n}Bu, R' = ^{i}Pr
Pn = Sb, R = Ph, R' = $SiMe_3$
Pn = Bi, R = ^{n}Bu, R' = ^{i}Pr

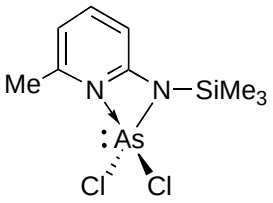

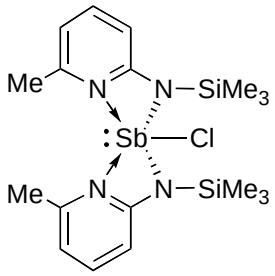

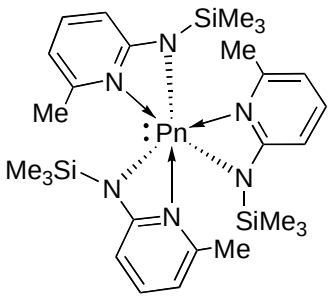

Pn = Sb, Bi

b)

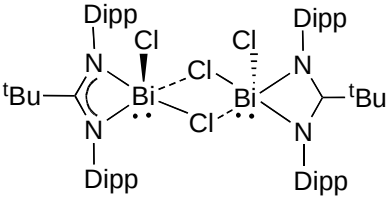

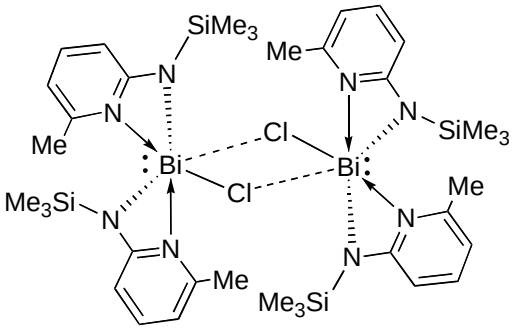

c)

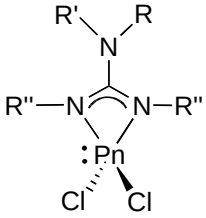

Pn = P, R = R' = Cy, R'' = Dipp
Pn = As, R = R' = Cy, R'' = Dipp
Pn = As, R = R' = ^{i}Pr, R'' = Dipp
Pn = As, R = H, R' = R'' Mes
Pn = Sb, R = R' = Cy, R'' = Dipp

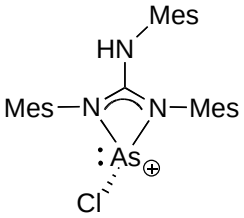

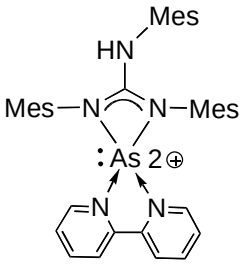

d)

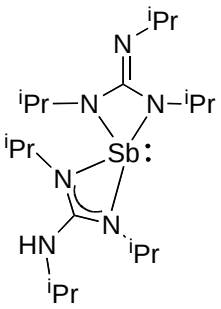

In this context, we report the first synthesis and comprehensive characterization of a series of chlorophosphines supported by homo- and heteroleptic (dianionic)guanidinates. The reactivity of the model compound tris(2,4,6-trimethylphenyl)guanidinato chlorophosphine (2,4,6-trimethylphenyl = Mes) has been studied extensively. We have explored the tendency of these compounds to retain the halogen

and therefore the reluctancy to form the "free" NHP. A base-stabilized NHP however was easily accessible and computational analysis has provided insight on this rather counterintuitive result and gave valuable data on the nature of the electronics about the phosphorus atom, and why these particular systems are resistant to halide abstraction. Novel chemically instigated carbodiimide elimination was observed in conjuction with metal coordination, resulting in the first structurally characterized metal complex with a cationic iminophosphine ligand. A study between chlorophosphine and a gentle one-electron reductant was explored to give the clean synthesis of the reductively coupled product featuring a dimeric structure with μ-*N,N′* bridging guanidinates and a P–P bond. Upon investigating the thermal stability of the tris(Mes)guanidinato chlorophosphine we discovered the thermally induced ejection of carbodiimide and subsequent insertion of chloro(imino)phosphine into the P–N bond of the initial diaminochlorophosphine resulting in a new ring expansion product with a μ-*N,N′* bridging guanidinate and a μ-bridging N-Mes. This ring expansion chemistry is extremely rare within P(III)–N chemistry. These observations collectively give a deeper perception on the nature and reactivity of diaminochlorophosphines constrained in a four-membered ring.

Experimental Section

General Procedures. All manipulations were performed in an inert atmosphere in a nitrogen filled MBraun Labmaster dp glovebox or using standard Schlenk techniques unless stated otherwise. Reagents were obtained from commercial sources. Triethylamine was distilled from CaH_2, phosphorus(III) chloride and phosphorus(III) bromide were distilled prior to use, while all other reagents were used without further purification. All solvents were dried using an MBraun controlled atmospheres solvent purification system and stored in Straus flasks under an N_2 atmosphere or over 4 Å molecular sieves in the glovebox. Chloroform-d was dried over CaH_2, distilled prior to use, and stored in the glovebox over 4 Å molecular sieves. The synthesis of *N,N′*-bis(2,6-diisopropylphenyl)carbodiimide (2,6-diisopropylphenyl = Dipp),[46] *N,N′*-bis(Mes)carbodiimide,[46] *N,N′,N″*-tris(Mes)guanidine[44] (**1**), *N,N′,N″*-tris(Dipp)guanidine[47] (**2**), *N,N′,N″*-tris(cyclohexyl)guanidine[48] (**5**) followed literature procedures. ^{1}H,

$^{13}C\{^{1}H\}$, $^{19}F\{^{1}H\}$ and $^{31}P\{^{1}H\}$ data were collected on a 400 MHz Varian Inova spectrometer (399.762 MHz for ^{1}H, 100.52 MHz for ^{13}C, 376.15 for ^{19}F and 161.825 MHz for ^{31}P). Spectra were recorded at room temperature (rt), unless otherwise indicated, in $CDCl_3$ using the residual protons of the deuterated solvent for reference and are listed in ppm, coupling constants are listed in Hz. Phosphorus and fluorine NMR spectra were recorded unlocked relative to an external standard (85% H_3PO_4, $\delta_P = 0.00$; $CF_3C_6H_5$, $\delta_F = -63.9$). Single crystal X-ray diffraction data were collected on a Nonius Kappa-CCD area detector or a Bruker Apex II-CCD detector using Mo-Kα radiation (λ = 0.71073 Å) and at a temperature of 150(2) K. Crystals were selected under Paratone-N oil, mounted on MiTeGen micromounts or nylon loops then immediately placed in a cold stream of N_2. Structures were solved and refined using SHELXTL. FT-IR spectra were collected on samples as KBr pellets using a Bruker Tensor 27 spectrometer, with a resolution of 4 cm^{-1}. Samples for FT-Raman spectroscopy were packed in capillary tubes and flame-sealed. Data was collected using a Bruker RFS 100/S spectrometer, with a resolution of 4 cm^{-1}. Melting (mp) and decomposition (dp) points were recorded in flame sealed capillary tubes using a Gallenkamp Variable Heater. High resolution mass spectrometry (HRMS) was collected using a Finnigan MAT 8200 instrument.[49] Elemental analyses (C, H, N) were performed by Laboratoire d'Analyse Élémentaire de l'Université de Montréal, Montréal, QC, Canada.

Synthesis. *General synthesis for guanidine*. After cooling a THF solution (15 mL) of aniline to 0 °C *n*-butyllithium (^{n}BuLi) was added to the cooled solution and stirred for 20 min. The yellow solution was allowed to warm to room temperature (rt). A THF solution (6 mL) of carbodiimide was added to the solution *via* cannula transfer causing the solution to turn orange. The reaction mixture was refluxed for 2 h. After cooling to rt, H_2O (1.5 mL) was added dropwise, resulting in a white precipitate from the dark orange solution. The reaction mixture was dried over $MgSO_4$ and filtered. The filtrate was dried by rotary evaporation, resulting in an orange wax. Recrystallization from hexanes at -30 °C yielded a white powder.

Specific procedures for guanidines.

3. Prepared from 2,6-diisopropylaniline (90%, 2.3 mL, 11.0 mmol), ^{n}BuLi (2.0 M in cyclohexane, 6.6 mL, 13.2 mol) and *N,N′*-bis(Mes)carbodiimide (3.06 g, 11.0 mmol). Yield: 58%; mp: 146-149 °C. X-ray quality colorless crystals were obtained from a concentrated CH_3CN solution after 8 days at -20 °C. ^{1}H NMR: δ 7.33-7.10 (3H, *aryl*), 7.00-6.86 (4H, *aryl*), 5.00 (br, 1H, N*H*), 4.78-4.71 (3s, 1H, N*H*), 3.63-3.37 (m, 2H, C*H*$(CH_3)_2$), 2.41 (d, 3H, CH(C*H*$_3)_2$, $^{3}J_{H\text{-}H}$ = 4.8), 2.37 (d, 3H, CH(C*H*$_3)_2$, $^{3}J_{H\text{-}H}$ = 6.0), 2.30 (s, 3H, C*H*$_3$), 2.25 (s, 3H, C*H*$_3$), 1.39 (d, 3H, CH(C*H*$_3)_2$, $^{3}J_{H\text{-}H}$ = 6.8), 1.35 (d, 3H, CH(C*H*$_3)_2$, $^{3}J_{H\text{-}H}$ = 7.2), 1.11 (m, 3H, C*H*$_3$). ^{13}C{^{1}H} NMR: δ 148.3, 147.2, 146.9, 146.4, 145.5, 144.4, 144.2, 144.0, 141.2, 137.8, 137.6, 136.6, 136.5, 136.3, 133.5, 133.3, 133.2, 132.3, 132.2, 130.9, 129.7, 129.6, 129.2, 129.1, 128.9, 127.9, 123.9, 123.4, 123.0, 122.4, 28.5, 28.1, 25.1, 24.0, 23.5, 22.5, 21.1, 20.9, 18.8, 18.6. FT-IR (cm^{-1} (ranked intensity)) 551(10), 693(11), 757(6), 799(8), 863(4), 1034(12), 1104(13), 1151(14), 1222(9), 1292(7), 1378(15), 1473(5), 1650(1), 2963(2), 3399(3). FT-Raman (cm^{-1} (ranked intensity)) 142(5), 236(14), 266(13), 572(3), 689(12), 883(15), 1159(10), 1255(8), 1306(6), 1381(4), 1444(11), 1608(2), 1650(7), 2867(9), 2919(1). HRMS: $C_{31}H_{41}N_3$ calcd (found) 455.3300 (455.3298). Elemental analysis: Calc for $C_{31}H_{41}N_3$: C 81.71, H 9.07, N 9.22; found C 81.23, H 9.28, N 9.28.

4. Prepared from 2,4,6-trimethylaniline (1.4 mL, 9.96 mmol), ^{n}BuLi (2.0 M in cyclohexane, 6.0 mL, 12.0 mmol) and *N,N′*-bis(Dipp)carbodiimide (3.58 g, 9.87 mmol). Yield: 33%; mp: 156-160 °C. X-ray quality colorless crystals were obtained from a concentrated CH_3CN solution after 5 days at -20 °C. ^{1}H NMR: δ 7.33-7.11 (5H, *aryl*), 7.01-6.86 (3H, *aryl*), 5.00 (s, 1H, N*H*), 4.74 (br, 1H, N*H*), 3.64-3.36 (m, 4H, C*H*$(CH_3)_2$), 2.42 (s, 2H, C*H*$_3$), 2.36 (s, 2H, C*H*$_3$), 2.29 (s, 3H, C*H*$_3$), 2.25 (d, 2H, CH(C*H*$_3)_2$, $^{3}J_{H\text{-}H}$ = 9.2), 1.38-1.04 (24H, C*H*$_3$). ^{13}C{^{1}H} NMR: δ 148.4, 148.3, 147.4, 147.3, 147.2, 146.3, 145.6, 144.2, 143.9, 141.5, 141.1, 137.8, 136.8, 136.4, 133.8, 133.5, 132.8, 132.5, 132.2, 131.7, 130.9, 129.7, 129.0, 128.9, 127.9, 127.7, 124.1, 123.8, 123.5, 123.1, 123.0, 122.5, 28.9, 28.8, 28.6, 28.5, 28.4, 28.0, 25.8, 25.3, 24.8, 24.1, 23.6, 23.1, 23.0, 22.2, 21.0, 20.8, 18.5, 18.3. FT-IR (cm^{-1} (ranked intensity)) 764(5), 800(8), 849(7), 935(10), 1059(15), 1109(9), 1255(13), 1295(6), 1361(11), 1383(14),

1493(4), 1586(12), 1647(1), 2962(2), 3409(3). FT-Raman (cm^{-1} (ranked intensity)) 147(6), 275(8), 445(14), 574(3), 676(9), 884(15), 1046(13), 1108(11), 1261(4), 1308(10), 1382(12), 1444(5), 1588(2), 2866(7), 2917(1). HRMS: $C_{34}H_{47}N_3$ calcd (found) 497.3770 (497.3771). Elemental analysis: Calc for $C_{34}H_{47}N_3$: C 82.04, H 9.52, N 8.44; found C 81.93, H 9.47, N 8.46.

1PCl. To a toluene solution (30 mL) of **1** (2.64 g, 6.39 mmol), PCl_3 (0.72 mL, 8.31 mmol) and NEt_3 (2.30 mL, 16.5 mmol) were added sequentially. The cloudy reaction mixture was stirred at rt for 2.5 h. The reaction mixture was cannula transferred to a Schlenk filter frit and the yellow filtrate was dried *in vacuo* to give a yellow powder. The powder was dissolved in CH_2Cl_2 (2 mL) and CH_3CN (5 mL) was added with vigorous stirring to precipitate a white powder. The suspension was centrifuged and the yellow solution decanted. This process was repeated and the decanted solutions were combined and placed in the freezer (-30 °C) for 30 min, during which, more white powder precipitated. The solution was decanted and the powder was dissolved in CH_2Cl_2 (2 mL) and added to those collected by centrifugation. The volatiles were removed *in vacuo* to give **1PCl** as a white powder (2.11 g, 4.42 mmol). Yield: 69%; mp: 143-146 °C. Single crystals suitable for X-ray diffraction experiments were grown by diffusion of CH_3CN into a concentrated CH_2Cl_2 solution of the bulk material at -30 °C for 4 weeks. ^1H NMR (-30 °C)[50]: δ 6.87 (s, 2H, *aryl*), 6.77 (s, 2H, *aryl*), 6.57 (s, 1H, *aryl*), 6.24 (s, 1H, *aryl*), 2.49 (s, 6H, C*H*$_3$), 2.41 (s, 6H, C*H*$_3$), 2.26 (s, 3H, C*H*$_3$), 2.22 (s, 6H, C*H*$_3$), 2.02 (s, 3H, C*H*$_3$), 1.88 (s, 3H, C*H*$_3$). $^{13}C\{^1H\}$ NMR (-30 °C)[50]: δ 144.8 (d, $^2J_{13C\text{-}P}$ = 6.0), 138.5, 138.3, 137.8, 135.9 (br), 131.3, 130.0, 129.2, 128.9 (d, $^2J_{13C\text{-}P}$ = 5.3), 128.0, 127.7 (d, $^3J_{13C\text{-}P}$ = 3.7), 127.3, 127.2, 21.1, 20.7, 20.3, 19.9 (br), 19.1, 18.4. $^{31}P\{^1H\}$ NMR: δ 181.1 (s). FT-IR (cm^{-1} (ranked intensity)) 448(6), 562(8), 682(10), 714(15), 756(11), 849(4), 948(14), 986(3), 1173(13), 1263(2), 1312(9), 1480(5), 1608(12), 1720(1), 2915(7). FT-Raman (cm^{-1} (ranked intensity)) 120(9), 193(11), 225(14), 253(7), 391(15), 448(8), 574(1), 1008(12), 1347(5), 1381(6), 1485(10), 1610(3), 1716(4), 2916(2), 3018(13). Elemental analysis: Calc for $C_{28}H_{33}N_3PCl$: C 70.35, H 6.96, N 8.79; found C 69.32, H 7.18, N 8.65.

General synthesis for halophosphine. To a toluene solution (20 mL) of guanidine (**1**-**5**), 1.3 and 2.6 equivalents of PCl_3 and NEt_3 were added, respectively in a sequential fashion. The reaction mixture was left to stir at rt overnight, during which time the solution became cloudy. Volatiles were removed *in vacuo* giving an off-white solid, which was resuspended in THF. The white solid was removed by centrifugation, and the liquid was concentrated *in vacuo* to give an off-white solid. The product was washed with CH_3CN (2 x 4 mL), decanting the colored solution each time. The product was dried *in vacuo* to give a white solid.

Specific procedures for halophosphines.

2PCl. Prepared from **2** (0.75 g, 1.39 mmol), PCl_3 (0.16 mL, 1.83 mmol) and NEt_3 (0.50 mL, 3.59 mmol). Yield: 72%; mp: 127-130 °C. X-ray quality colorless crystals were obtained from a concentrated CH_2Cl_2 solution after four weeks at -20 °C. ^{1}H NMR (-30 °C)[50]: δ 7.30 (t, 2H, *aryl*, $^3J_{H\text{-}H}$ = 7.6), 7.22 (d, 2H, *aryl*, $^3J_{H\text{-}H}$ = 7.6), 7.13 (m, 2H, *aryl*), 7.00 (d, 1H, *aryl*, $^3J_{H\text{-}H}$ = 7.6), 6.81 (t, 1H, *aryl*, $^3J_{H\text{-}H}$ = 7.6), 6.61 (d, 1H, *aryl*, $^3J_{H\text{-}H}$ = 7.6), 3.42 (m, 4H, C*H*$(CH_3)_2$), 3.31 (br sept, 1H, C*H*$(CH_3)_2$), 2.47 (br sept, 1H, C*H*$(CH_3)_2$), 1.41 (d, 6H, CH(C*H*$_3)_2$, $^3J_{H\text{-}H}$ = 6.4), 1.32 (d, 6H, CH(C*H*$_3)_2$, $^3J_{H\text{-}H}$ = 6.8), 1.26 (d, 6H, CH(C*H*$_3)_2$, $^3J_{H\text{-}H}$ = 6.8), 1.18 (m, 9H, CH(C*H*$_3)_2$), 0.86 (d, 6H, CH(C*H*$_3)_2$, $^3J_{H\text{-}H}$ = 6.4), 0.56 (d, 6H, CH(C*H*$_3)_2$, $^3J_{H\text{-}H}$ = 6.0). ^{13}C{^{1}H} NMR (-30 °C)[50]: δ 149.5, 147.5, 141.3 (d, $^2J_{13C\text{-}P}$ = 5.6), 140.0, 138.5, 137.4, 130.6 (d, $^2J_{13C\text{-}P}$ = 4.8), 128.8, 124.1, 124.0, 123.4, 123.0, 121.2, 30.1, 30.0, 28.9, 28.2, 27.4, 27.3, 23.6, 23.3, 22.9, 22.6, 22.4. ^{31}P{^{1}H} NMR: δ 179.9 (s). FT-IR (cm^{-1} (ranked intensity)) 527(15), 674(11), 752(8), 786(4), 984(3), 1121(10), 1219(7), 1260(5), 1323(9), 1363(14), 1386(12), 1438(6), 1588(13), 1717(1), 2965(2). FT-Raman (cm^{-1} (ranked intensity)) 137(6), 279(9), 451(13), 887(5), 1048(15), 1104(12), 1252(14), 1299(10), 1353(8), 1443(4), 1589(1), 1718(3), 2867(7), 2909(2), 3062(11). Elemental analysis: Calc for $C_{37}H_{51}N_3PCl$: C 73.55, H 8.51, N 6.95; found C 72.69, H 8.66, N 6.90.

3PCl. Synthesized from **3** (1.10 g, 2.42 mmol), PCl_3 (0.27 mL, 3.12 mmol) and NEt_3 (0.87 mL, 6.25 mmol). Yield: 35%; mp: 142-146 °C. X-ray quality colorless crystals were obtained after three

days from a concentrated hexanes solution at -20 °C. ^{1}H NMR (-30 °C)[50]: δ 7.38 (t, 1H, *aryl*, $^{3}J_{H\text{-}H}$ = 7.6), 7.30 (d, 1H, *aryl*, $^{3}J_{H\text{-}H}$ = 7.6), 7.26 (d, 1H, *aryl*, $^{3}J_{H\text{-}H}$ = 7.6), 6.76 (s, 1H, *aryl*), 6.58 (s, 1H, *aryl*), 6.54 (s, 1H, *aryl*), 6.25 (s, 1H, *aryl*), 3.81 (sept, 1H, C*H*CH$_3$, $^{3}J_{H\text{-}H}$ = 6.4), 3.42 (sept, 1H, C*H*CH$_3$, $^{3}J_{H\text{-}H}$ = 6.8), 2.49 (s, 3H, C*H*$_3$), 2.27 (s, 3H, C*H*$_3$), 2.21 (s, 3H, C*H*$_3$), 2.15 (s, 3H, C*H*$_3$), 2.02 (s, 3H, C*H*$_3$), 1.90 (s, 3H, C*H*$_3$), 1.38 (m, 9H, CHC*H*$_3$), 1.32 (d, 3H, CHC*H*$_3$, $^{3}J_{H\text{-}H}$ = 6.8). ^{13}C{^{1}H} NMR (-30 °C)[50]: δ 150.2, 148.1, 145.5 (d, $^{2}J_{13C\text{-}P}$ = 5.9), 138.4, 137.6, 137.1, 134.6, 131.4, 130.2, 129.2, 129.1 (d, $^{2}J_{13C\text{-}P}$ = 2.8), 128.95, 128.9, 128.6, 128.1, 127.8, 127.3, 124.4, 123.9, 29.5 (d, $J_{13C\text{-}P}$ = 4.2), 28.8, 25.8, 25.5 (d, $J_{13C\text{-}P}$ = 4.8), 24.6, 24.3, 21.0, 20.7, 20.1 (d, $J_{13C\text{-}P}$ = 9.9), 19.8, 19.1, 18.3. ^{31}P{^{1}H} NMR: δ 180.5 (s). FT-IR (cm^{-1} (ranked intensity)) 462(4), 561(13), 681(10), 714(15), 767(9), 803(5), 846(12), 985(6), 1227(11), 1266(2), 1317(8), 1466(7), 1608(14), 1698(1), 2963(3). FT-Raman (cm^{-1} (ranked intensity)) 97(15), 143(7), 226(6), 461(8), 575(2), 1009(14), 1316(10), 1358(5), 1455(9), 1590(12), 1609(4), 1701(3), 2863(11), 2917(1), 2964(13).

4PCl. **4** (0.75 g, 1.51 mmol), PCl_3 (0.17 mL, 1.96 mmol) and NEt_3 (0.55 mL, 3.92 mmol). Yield: 61%; mp: 138-141 °C. X-ray quality colorless crystals were obtained after two weeks from a concentrated CH_2Cl_2/Et_2O solution at -20 °C. ^{1}H NMR (-30 °C)[50]: δ 7.43 (t, 1H, *aryl*, $^{3}J_{H\text{-}H}$ = 7.6), 7.34 (d, 1H, *aryl*, $^{3}J_{H\text{-}H}$ = 7.6), 7.30 (d, 1H, *aryl*, $^{3}J_{H\text{-}H}$ = 7.6), 6.92 (d, 1H, *aryl*, $^{3}J_{H\text{-}H}$ = 7.2), 6.78 (s, 1H, *aryl*), 6.75 (t, 1H, *aryl*, $^{3}J_{H\text{-}H}$ = 7.6), 6.53 (d, 1H, *aryl*), 6.51 (s, 1H, *aryl*), 3.80 (sept, 1H, C*H*(CH$_3$)$_2$, $^{3}J_{H\text{-}H}$ = 6.8), 3.39 (m, 2H, C*H*(CH$_3$)$_2$), 2.94 (sept, 1H, C*H*(CH$_3$)$_2$, $^{3}J_{H\text{-}H}$ = 6.4), 2.47 (s, 3H, C*H*$_3$), 2.15 (s, 3H, C*H*$_3$), 2.13 (s, 3H, C*H*$_3$), 1.41 (m, 9H, CH(C*H*$_3$)$_2$), 1.35 (d, 3H, CH(C*H*$_3$)$_2$, $^{3}J_{H\text{-}H}$ = 6.4), 1.32 (d, 3H, CH(C*H*$_3$)$_2$, $^{3}J_{H\text{-}H}$ = 6.8), 0.95 (m, 6H, CH(C*H*$_3$)$_2$), 0.83 (d, 3H, CH(C*H*$_3$)$_2$, $^{3}J_{H\text{-}H}$ = 6.4). ^{13}C{^{1}H} NMR (-30 °C)[50]: δ 150.7, 148.4, 142.7 (d, $^{2}J_{13C\text{-}P}$ = 5.6), 139.7, 138.6, 138.3, 137.1, 137.0, 134.4, 130.3, 129.5 (d, $^{2}J_{13C\text{-}P}$ = 4.0), 129.0, 128.95, 128.9, 124.2, 123.6, 122.7, 121.6, 120.6, 29.5 (d, $J_{13C\text{-}P}$ = 2.9), 29.0, 28.9, 28.4, 26.5 (d, $J_{13C\text{-}P}$ = 8.0), 26.4, 25.2, 24.9, 24.1, 23.9, 21.2, 21.0, 20.5, 19.8 (d, $J_{13C\text{-}P}$ = 10.9), 19.2. ^{31}P{^{1}H} NMR: δ 178.6 (s). FT-IR (cm^{-1} (ranked intensity)) 432(11), 461(9), 558(15), 675(12), 754(5), 782(7), 883(14), 986(4), 1268(3), 1317(8), 1362(13), 1465(6), 1587(10), 1705(1), 2965(2). FT-

Raman (cm^{-1} (ranked intensity)) 109(9), 200(14), 462(8), 578(5), 625(11), 887(7), 1011(13), 1259(10), 1319(12), 1360(4), 1448(6), 1590(2), 1708(3), 2925(1), 3065(15). Elemental analysis: Calc for $C_{34}H_{45}N_3PCl$: C 72.64, H 8.07, N 7.47; found C 71.97, H 8.06, N 7.37.

5PCl. **5** (0.55 g, 1.80 mmol), PCl_3 (0.20 mL, 2.34 mmol), NEt_3 (0.65 mL, 4.68 mmol). Yield: 31%; mp: 75-78 °C. ^1H NMR (-30 °C)[50]: δ 3.53-3.35 (m, 3H, C*H*), 2.10-2.01 (m, 4H, CH_2), 1.82-1.14 (m, 26H, CH_2). ^{13}C NMR (-30 °C)[50]: δ 145.6, 55.9, 54.5, 51.4, 35.5, 35.3, 33.6, 33.5, 33.4, 32.1, 31.8, 25.61, 25.56, 25.4, 25.2, 25.1, 25.0. ^{31}P NMR: δ 181.5 (s). FT-IR (cm^{-1} (ranked intensity)) 433(7), 655(3), 699(8), 725(14), 839(10), 890(9), 988(4), 1109(13), 1148(12), 1215(5), 1298(11), 1361(15), 1449(6), 1704(2), 2930(1). FT-Raman (cm^{-1} (ranked intensity)) 85(8), 143(14), 216(6), 430(10), 659(13), 728(12), 811(7), 1027(9), 1253(11), 1347(15), 1444(4), 1702(3), 2854(2), 2887(5), 2938(1). Elemental analysis: Calc for $C_{19}H_{33}N_3PCl$: C 61.69, H 8.99, N 11.36; found C 61.35, H 9.26, N 11.17.

1PBr. **1** (0.93 g, 2.24 mmol), PCl_3 (0.27 mL, 2.92 mmol), NEt_3 (0.81 mL, 5.81 mmol). Yield: 70%; mp: 117-123 °C. Single crystals suitable for X-ray diffraction experiments were grown by diffusion of CH_3CN into a concentrated CH_2Cl_2 solution of the bulk material at -30 °C for 3 days. ^1H NMR (-30 °C)[50]: δ 6.88 (s, 2H, *aryl*), 6.79 (br s, 2H, *aryl*), 6.61 (s, 1H, *aryl*), 6.26 (s, 1H, *aryl*), 2.49 (s, 6H, CH_3), 2.47 (br s, 6H, CH_3), 2.29 (s, 3H, CH_3), 2.24 (s, 6H, CH_3), 2.04 (s, 3H, CH_3), 1.89 (s, 3H, CH_3). $^{13}C\{^1H\}$ NMR (-30 °C)[50]: δ 144.1 (d, $^2J_{13C\text{-}P}$ = 5.13 Hz), 138.2, 137.8, 135.6, 131.4, 129.8, 129.4, 129.0, 127.9, 127.8, 127.3, 21.1, 20.7, 20.3, 19.9, 19.8, 19.3, 18.3. $^{31}P\{^1H\}$ NMR: δ 200.2 (s). FT-IR (cm^{-1} (ranked intensity)) 414(15), 559(7), 674(11), 756(9), 803(14), 849(6), 951(12), 983(3), 1268(2), 1315(8), 1374(13), 1478(4), 1609(10), 1698(1), 2916(5). FT-Raman (cm^{-1} (ranked intensity)) 97(8), 147(4), 177(15), 207(12), 240(9), 324(7), 413(13), 570(2), 1010(14), 1358(6), 1379(11), 1489(10), 1610(3), 1700(1), 2918(5). Elemental analysis: Calc for $C_{28}H_{33}N_3PBr$: C 64.37, H 6.37, N 8.04; found C 64.06, H 6.42, N 7.93.

General synthesis for ***6M****, M = Al, Ga.* To a CH_2Cl_2 solution (5 mL) of **1PCl**, a CH_2Cl_2 solution (3 mL) of MCl_3 was added slowly with stirring. In all cases the reaction mixtures turned yellow. The

reactions were stirred at rt for 3 h, during which time the yellow color became less intense. The volatiles were removed *in vacuo* to give slightly yellow powders.

6Al. Compound **6Al** was prepared from **1PCl** (0.20 g, 0.41 mmol) and $AlCl_3$ (0.055 g, 0.41 mmol). The crude product was purified by liquid diffusion of hexane into a concentrated CH_2Cl_2 solution of the bulk powder at -30 °C for 48 h. This gave a microcrystalline white powder. Yield: 53%; dp: 160-164 °C. X-ray quality crystals were obtained from slow evaporation of a concentrated CH_2Cl_2 solution of the bulk powder at rt for a two week period. ^{1}H NMR: δ 7.02 (s, 1H, *aryl*), 7.00 (s, 1H, *aryl*), 6.76 (s, 1H, *aryl*), 6.68 (s, 1H, *aryl*), 6.52 (s, 1H, *aryl*), 6.19 (s, 1H, *aryl*), 2.72 (s, 3H, C*H*$_3$), 2.64 (s, 3H, C*H*$_3$), 2.55 (s, 3H, C*H*$_3$), 2.51 (d, 3H, C*H*$_3$ $J_{H\text{-}P}$ = 2.0), 2.35 (s, 3H, C*H*$_3$), 2.20 (s, 3H, C*H*$_3$), 2.11 (s, 3H, C*H*$_3$), 2.07 (s, 6H, C*H*$_3$). ^{13}C{^{1}H} NMR: δ 160.8 (d, $^2J_{13C\text{-}P}$ = 9.95), 140.8, 140.0, 139.0, 138.8, 137.7, 137.3, 136.6, 135.3, 133.6, 133.3, 130.5, 130.2, 130.0, 129.6, 129.0, 128.5, 127.3, 21.4, 21.3 (d, $J_{13C\text{-}P}$ = 7.34), 21.0, 20.9, 20.8, 20.7, 20.6, 20.3, 19.2. ^{31}P{^{1}H} NMR: δ 171.4 (s). FT-IR (cm^{-1} (ranked intensity)) 412(14), 429(9), 471(11), 505(2), 661(6), 711(10), 748(4), 855(3), 885(15), 981(8), 1195(12), 1282(5), 1352(13), 1555(1), 2922(7). FT-Raman (cm^{-1} (ranked intensity)) 186(7), 221(9), 283(10), 430(8), 495(5), 574(2), 661(13), 1018(14), 1321(12), 1352(4), 1386(6), 1482(11), 1609(3), 2925(1), 3024(15).

6Ga. Compound **6Ga** was synthesized from **1PCl** (0.25 g, 0.52 mmol) and $GaCl_3$ (0.093 g, 0.53 mmol). The crude product was purified by redissolving in CH_2Cl_2 and precipitating white solids by the addition of hexanes with rapid stirring. The solution was decanted and the white product was dried *in vacuo*. Yield: 66%; dp: 171-179 °C. ^{1}H NMR: δ 7.02 (s, 1H, *aryl*), 7.01 (s, 1H, *aryl*), 6.75 (s, 1H, *aryl*), 6.68 (s, 1H, *aryl*), 6.51 (s, 1H, *aryl*), 6.20 (s, 1H, *aryl*), 2.73 (s, 3H, C*H*$_3$), 2.65 (s, 3H, C*H*$_3$), 2.53 (s, 3H, C*H*$_3$), 2.51 (d, 3H, C*H*$_3$ $J_{H\text{-}P}$ = 2.4), 2.35 (s, 3H, C*H*$_3$), 2.20 (s, 3H, C*H*$_3$), 2.07 (virtual d, 9H, C*H*$_3$). ^{13}C{^{1}H} NMR: δ 159.7 (d, $^2J_{13C\text{-}P}$ = 10.3), 140.8, 139.9, 139.0, 138.8, 137.9, 137.4, 136.5, 135.3, 133.4, 133.3, 130.7, 130.1 (d, $^3J_{13C\text{-}P}$ = 3.32), 130.06, 129.6, 129.4, 129.0, 128.4, 127.0 (d, $^3J_{13C\text{-}P}$ = 1.81), 21.4, 21.2 (d, $J_{13C\text{-}P}$ = 3.22), 21.0, 20.9, 20.8, 20.7, 20.6, 20.1, 19.2. ^{31}P{^{1}H} NMR: δ 172.7 (s).

FT-IR (cm^{-1} (ranked intensity)) 463(15), 493(2), 552(5), 657(9), 705(14), 750(7), 855(3), 980(8), 1280(4), 1321(10), 1352(12), 1477(6), 1560(1), 1611(13), 2921(11). FT-Raman (cm^{-1} (ranked intensity)) 199(6), 241(13), 360(4), 388(11), 493(7), 573(2), 657(15), 1017(12), 1321(10), 1352(5), 1385(8), 1482(9), 1609(3), 2924(1), 3023(14). Elemental analysis: Calc for $C_{28}H_{33}N_3PCl_4Ga$: C 51.41, H 5.09, N 6.42; found C 50.95, H 5.31, N 6.32.

7. A CH_2Cl_2 solution (8 mL) of **1PCl** (0.35 g, 0.73 mmol) was added to solid $Pt(PPh_3)_4$ (0.91 g, 0.73 mmol) to give a clear orange solution. After stirring at rt for 45 min Me_3SiOTf was added and the color changed instantly to dark red. The volatiles were removed after stirring at rt for 30 min resulting in a waxy brown product. Hexanes washes (3 x 5 mL) yielded a brown powder. The bulk material was dissolved in CH_2Cl_2 (3 mL) and stirred vigorously as hexanes (8 mL) were added leading to the precipitation of brown powder. The supernatant was decanted and discarded and the bulk material once again dissolved in CH_2Cl_2 (3 mL) and set up for recrystallization by layering hexanes (6 mL) and keeping at -30 °C for 4 days. Yield: 56%; dp: 87-92 °C. ^1H NMR: δ 7.34 (t, 9H, *aryl*, $^3J_{H\text{-}H}$ = 8.0), 7.07 (t, 18H, *aryl*, $^3J_{H\text{-}H}$ = 8.0), 6.94 (d, 18H, *aryl*, $^3J_{H\text{-}H}$ = 8.0), 6.68 (s, 2H, *aryl*), 2.15 (s, 3H, C*H*$_3$), 1.67 (s, 6H, C*H*$_3$). $^{13}C\{^1H\}$ NMR: δ 133.5, 131.0, 129.0, 128.9, 21.6, 19.2. $^{31}P\{^1H\}$ NMR: δ 147.0 (br t), 23.3 ($^2J_{P\text{-}P}$ = 65, $^1J_{P\text{-}195Pt}$ = 3990). $^{19}F\{^1H\}$ NMR: δ -78.3 (s). FT-IR (cm^{-1} (ranked intensity)) 418(12), 516(2), 637(7), 694(1), 744(5), 853(13), 998(14), 1030(6), 1092(9), 1147(10), 1222(15), 1272(3), 1435(4), 1480(8), 3054(11). FT-Raman (cm^{-1} (ranked intensity)) 97(8), 244(4), 313(13), 415(11), 618(15), 1001(2), 1029(10), 1075(12), 1094(9), 1302(7), 1382(14), 1492(1), 1585(6), 1605(3), 3059(5). Elemental analysis: Calc for $C_{64}H_{56}F_3NO_3P_4PtS$: C 59.35, H 4.36, N 1.08; found C 59.04, H 4.42, N 1.07.

8. To a CH_2Cl_2 solution (5 mL) of **1PCl** (0.40 g, 0.83 mmol) was added a CH_2Cl_2 solution (2 mL) of 2,2'-bipyridine (0.13 g, 0.83 mmol) and Me_3SiOTf (150 μL, 0.83 mmol). The previously colorless solution turned yellow after the addition of Me_3SiOTf and was allowed to stir at rt for 3.5 h before removing the volatiles *in vacuo* to give an orange waxy product. Washing with hexanes (2 x 5 mL) produced an orange powder. The powder was redissolved in CH_2Cl_2 (3 mL) and hexanes (6 mL)

were added to produce an oil. The supernatant was decanted and the oil dried to give an orange powder. This process was repeated three times. Yield: 72%; dp: 128-133 °C. ^{1}H NMR: δ 9.22 (d, 2H, *bpy*, $^{3}J_{H\text{-}H}$ = 8.0), 8.59 (br d, 2H, *bpy*), 8.50 (t, 2H, *bpy*, $^{3}J_{H\text{-}H}$ = 8.0), 7.64 (br t, 2H, *bpy*), 2.76 (br s, 6H, C*H*$_3$), 2.21 (s, 6H, C*H*$_3$), 2.06 (s, 3H, C*H*$_3$), 1.99 (s, 3H, C*H*$_3$), 1.82 (br s, 6H, C*H*$_3$), 1.77 (s, 3H, C*H*$_3$). ^{13}C NMR: δ 146.6 (d, $^{2}J_{13C\text{-}P}$ = 5.0), 145.1, 144.6, 139.8, 138.1, 136.6, 136.1, 132.0, 131.3, 130.0, 128.8, 128.1, 127.8, 127.6 (d, $^{2}J_{13C\text{-}P}$ = 4.0), 125.8 (d, $^{2}J_{13C\text{-}P}$ = 5.0), 21.4, 21.0, 20.7, 19.8, 18.7, 18.5. ^{19}F NMR: δ -78.6. ^{31}P NMR: δ 106.0 (s). FT-IR (cm^{-1} (ranked intensity)) 476(14), 517(8), 564(12), 637(3), 724(13), 770(7), 854(10), 988(15), 1031(2), 1155(5), 1260(1), 1478(6), 1613(11), 1695(4), 2921(9). FT-Raman (cm^{-1} (ranked intensity)) 85(2), 394(14), 570(4), 633(13), 770(9), 1016(7), 1251(15), 1304(11), 1331(3), 1384(12), 1497(8), 1563(10), 1608(1), 1694(6), 2922(5).

9. A THF (3mL) solution of Cp_2Co (0.43 g, 2.27 mmol) was added to a colorless THF (3 mL) solution of **1PCl** (1.08 g, 2.27 mmol). The reaction mixture turned a dark brown color and after stirring for 48 h at rt copious amounts of green precipitate were visible. The green precipitate was separated by centrifugation and the dark solution was decanted and dried *in vacuo* to give an off-white solid. The product was washed with CH_3CN (2 x 6 mL) to remove remaining Cp_2Co and the suspension was centrifuged. The solid white product was dissolved in CH_2Cl_2 (3 mL) and precipitated with the addition of CH_3CN, the solution was decanted and discarded, and this process was repeated once more. After the second precipitation the vial was placed in the freezer (-30 °C) for 45 min, the slightly colored solution was discarded and the white precipitate was dried *in vacuo*. X-ray quality crystals were grown at -30 °C from the liquid diffusion of CH_3CN into a concentrated CH_2Cl_2 solution of the bulk material over a one-week period. Yield: 61%; dp: 310-320 °C. ^{1}H NMR (-50 °C)[50]: δ 6.95 (s, 2H, *aryl*), 6.80 (s, 2H, *aryl*), 6.63 (s, 2H, *aryl*), 6.42 (s, 2H, *aryl*), 6.10 (s, 2H, *aryl*), 5.96 (s, 2H, *aryl*), 2.82 (s, 6H, C*H*$_3$), 2.44 (s, 6H, C*H*$_3$), 2.39 (s, 6H, C*H*$_3$), 2.30 (s, 6H, C*H*$_3$), 2.22 (s, 6H, C*H*$_3$), 2.06 (s, 6H, C*H*$_3$), 1.98 (s, 6H, C*H*$_3$), 1.52 (s, 6H, C*H*$_3$), 1.48 (s, 6H, C*H*$_3$). ^{13}C{^{1}H} NMR (-50 °C)[50]: δ 146.2 (dd, $^{2}J_{13C\text{-}P}$ = 6.0), 142.2, 138.4, 138.2, 137.3 (br), 136.8, 135.8 (br), 134.5, 130.2 (br), 129.6 (br), 129.2, 128.3 (br), 128.1, 126.8 (dd,

$^{2}J_{13C\text{-}P}$ = 7.2), 125.6, 21.8, 21.3 - 20.8 (br), 20.6, 20.2 (br), 19.0 (d, $J_{13C\text{-}P}$ = 2.6), 18.7 (br). $^{31}P\{^{1}H\}$ NMR: δ 59.2 (s). FT-IR (cm^{-1} (ranked intensity)) 532(10), 562(7), 604(14), 719(5), 747(9), 848(6), 949(11), 1005(3), 1188(12), 1232(2), 1308(15), 1375(13), 1477(4), 1642(1), 2915(8). FT-Raman (cm^{-1} (ranked intensity)) 108(9), 243(14), 403(15), 430(10), 474(6), 531(11), 576(5), 968(12), 1019(13), 1220(8), 1307(4), 1381(7), 1609(1), 1660(3), 2915(2). Elemental analysis: Calc for $C_{56}H_{66}N_6P_2$: C 75.99, H 7.52, N 9.49; found C 75.67, H 7.44, N 9.47.

10. Compound **1PCl** (0.54 g, 1.1 mmol) was dissolved in toluene (6mL) and heated to 90 °C for 48 h. The solvent was removed *in vacuo* giving a colorless waxy material, which became a powder after stirring in pentane for 5 min. The solvent was decanted and the white powder was dried *in vacuo*. The product was further purified by recrystallization from slow diffusion of CH_3CN into a concentrated CH_2Cl_2 solution of the bulk material at -30 °C. Single crystals suitable for X-ray diffraction studies were grown in a similar fashion after 11 days in the freezer. Yield: 34%; mp: 178-182 °C. ^{1}H NMR: δ 6.94 (s, 4H, *aryl*), 2.64 (s, 12H, C*H*$_3$), 2.29 (s, 6H, C*H*$_3$). $^{13}C\{^{1}H\}$ NMR: δ 138.3, 138.1, 132.0, 129.8, 21.1, 19.6. $^{31}P\{^{1}H\}$ NMR: δ 211.0 (s). FT-IR (cm^{-1} (ranked intensity)) 408(2), 485(5), 511(7), 558(3), 600(10), 716(14), 896(1), 1035(13), 1158(9), 1218(6), 1263(11), 1308(15), 1375(12), 1476(4), 2916(8). FT-Raman (cm^{-1} (ranked intensity)) 181(14), 221(2), 379(3), 405(11), 486(10), 543(12), 577(4), 632(8), 984(15), 1274(6), 1317(1), 1386(9), 1482(13), 1612(5), 2920(7). HRMS for $C_{18}H_{22}N_2Cl_2P_2^{+}$ calc(found) 398.0635(398.0622). Elemental analysis: Calc for $C_{18}H_{22}Cl_2N_2P_2$: C 54.15, H 5.55, N 7.02; found C 53.97, H 5.51, N 6.92.

11. In a pressure tube **1PCl** (0.54 g, 1.1 mmol) was dissolved in $CDCl_3$ (3 mL) and heated in an oil bath at 90 °C overnight. The solvent was removed *in vacuo*, producing a wax-like colorless product. This was washed with pentane (6 mL), which produced a white powder. The suspension was centrifuged and the decanted solution was transferred to a vial and kept in the freezer (-35 °C) for 1 h. The centrifuged white solid was dissolved in CH_2Cl_2, transferred to a vial and dried *in vacuo* to give a sticky white solid. Resuspension in pentane and drying *in vacuo* produced a fine white powder. The

cooled solution had a white precipitate, which was isolated by decanting the pentane and drying *in vacuo* to give a white powder, which was combined with the previous isolated product. Single crystals suitable for X-ray diffraction studies were grown from a concentrated CH_3CN solution of the bulk material at -30 °C for two weeks. Yield: 33%; mp: 204-209 °C. ^{1}H NMR: δ 6.94 (br s, 2H, *aryl*), 6.88 (br s, 2H, *aryl*), 6.61 (br s, 2H, *aryl*), 6.30 (br s, 2H, *aryl*), 2.86 (s, 6H, C*H*$_3$), 2.56 (br s, 6H, C*H*$_3$), 2.35 (br s, 6H, C*H*$_3$), 2.27 (br s, 3H, C*H*$_3$), 2.22 (s, 3H, C*H*$_3$), 2.21 (s, 3H, C*H*$_3$), 2.04 (s, 3H, C*H*$_3$), 1.87 (s, 6H, C*H*$_3$). ^{13}C NMR: δ 141.9, 138.8, 138.7138.0, 137.9, 137.8, 137.7, 136.7, 136.6, 136.1, 135.9, 131.2, 130.2, 129.9, 129.0, 127.8, 126.7, 21.5, 21.4, 21.0, 20.9, 20.6, 20.5, 20.4, 19.7. ^{31}P NMR: δ 140.2 (s). FT-IR (cm^{-1} (ranked intensity)) 452(3), 563(9), 600(11), 722(15), 853(5), 950(7), 981(10), 1056(4), 1140(14), 1183(8), 1222(1), 1475(6), 1608(12), 1649(2), 2919(13). FT-Raman (cm^{-1} (ranked intensity)) 86(6), 204(7), 396(14), 421(8), 443(10), 511(15), 580(4), 1058(11), 1307(5), 1381(9), 1535(13), 1610(2), 1652(3), 2921(1), 3007(12). HRMS for $C_{37}H_{44}N_4Cl_2P_2^+$ calc(found) 676.2418(676.2413). Elemental analysis: Calc for $C_{37}H_{44}N_4Cl_2P_2$: C 65.58, H 6.54, N 8.27; found C 65.81, H 6.94, N 8.15.

Computational Details. All calculations were done with the program packages Turbomole 6.3[51] and ADF 2010.2.[52] Geometries of the studied systems were optimized using the PBE1PBE density functional[53-56] in combination with the def2-TZVP basis sets.[57,58] The nature of stationary points found was assessed by calculating full Hessian matrices at the respective level of theory. Partial atomic charges were calculated with the natural population analysis (NPA) as implemented in Turbomole 6.3.[59] The nature of phoshporus-chlorine interaction in the studied chlorophosphines was inspected with the energy decomposition analysis (EDA) procedure[60] as implemented in ADF 2010.2.[61-63] The analyses were performed at the PBE1PBE/def2-TZVP optimized geometries using the PBE1PBE density functional in together with the all electron Slater-type TZP basis sets.[64] The program gOpenMol was used for all visualizations of molecular structures and Kohn-Sham orbitals.[65,66]

Results and Discussions

Synthesis. Synthesis of *N,N′,N″*-tris(*aryl*)guanidines (**1**-**4**, *aryl* = Mes and Dipp) followed the literature procedure of Boeré *et al*.[47] Preparations were accomplished by refluxing *N,N′*-

bis(R)carbodiimide and lithium (R')anilide in THF for 2 h, the addition of water, gave either the homoleptic guanidines **1** and **2** (R = R' = Mes for **1**; R = R' = Dipp for **2**) or the heteroleptic guanidines **3** and **4** (R = Mes; R' = Dipp for **3**; R = Dipp; R' = Mes for **4**; Scheme 1). Upon removal of THF, compounds **3** and **4** deposited as wax like materials on the sides of the flask. Further recrystallization from hexanes produced white powders, which were sampled for analysis by proton NMR spectroscopy. Spectra of the isolated materials demonstrated dynamic behaviour indicative of sterically bulky guanidines.[47] These phenomena have been documented elsewhere (for **2**)[47] using variable temperature NMR spectroscopy and will not be discussed further (see ESI for sample spectra). Single crystals of **3** and **4** were grown from concentrated CH_3CN solutions of the bulk powder at -20 °C, and subsequent X-ray diffraction studies confirmed the synthesis of the heteroleptic guanidines in moderate to low yields (58 % and 33 %, respectively; see ESI for solid-state structures). Synthesis of *N,N′,N″*-tris(cyclohexyl)guanidine (**5**) followed the reported facile procedure of Richeson *et al.* where cyclohexylamine and *N,N′*-dicyclohexylcarbodiimide are combined and heated at 90 °C in hexane in a pressure tube for two days.[48]

Scheme 1. Synthetic route for *N,N′,N″*-tris(*aryl*)guanidines (**1**-**4**).

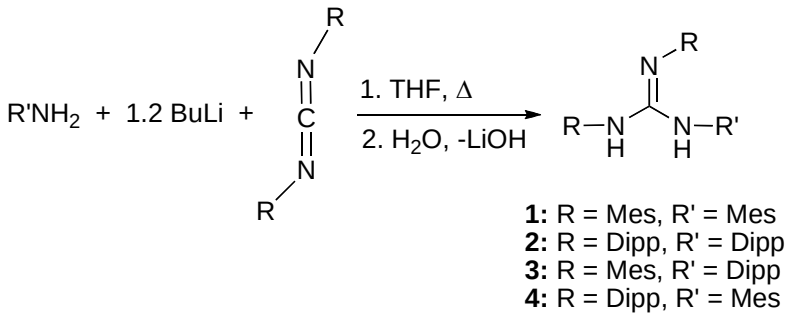

The sequential addition of PCl_3 and NEt_3 to a toluene solution of *N,N′,N″*-tris(*aryl*)guanidine (**1**-**4**) or *N,N′,N″*-tris(cyclohexyl)guanidine (**5**) (Scheme 2) in a 1.3:2.6:1 stochiometry at room temperature generated copious amounts of white precipitate. Aliquots of the reaction mixture were sampled every hour and analysed by $^{31}P\{^1H\}$ NMR spectroscopy, which in all cases showed the emergence of signals

shifted upfield from PCl_3, consistent with the chemical shifts reported for diaminochlorophosphines (δ_P = 178 – 181, Table 1; *cf.* δ_P = 102 – 210).[25,29,67-70] A distinct difference in reaction completion times emerged based on the steric bulk of the ligands; when the steric demand was increased, reaction times were correspondingly longer from 1 (**1**,**3**-**5**) to 12 (**2**) hours. Upon no further change in the $^{31}P\{^1H\}$ NMR spectra, the reaction mixtures were filtered or centrifuged. Removal of the volatiles of the supernatant *in vacuo* gave light yellow powders in all cases. Further washing of the powders with CH_3CN yielded white powders, which were sampled for multinuclear NMR spectroscopic analysis, where the $^{31}P\{^1H\}$ NMR spectra showed only a single peak identical to that observed for their respective reaction mixtures, with the exception of **3PCl**. The initial reaction mixture of **3PCl** taken after 1 h showed the emergence of two peaks (δ_P = 178 and 181) with equal intensities, no change was observed in the $^{31}P\{^1H\}$ NMR spectrum after continuing to monitor the reaction for 24 h. The purified product had a single resonance (δ_P = 181). The proton NMR spectrum of crude **3PCl** supported the conclusion that two products were present based on the extra resonances observed when compared to a spectrum of pure **3PCl** at δ_P = 181. Presumably the products at δ_P = 178 and 181 were the symmetric and asymmetric chelating guanidinates, respectively (Chart 4). Single crystals of the product with a phosphorus chemical shift of 181 ppm were grown, which confirmed an asymmetric chelating guanidinate (Chart 4b). In an attempt to isomerize to one product, an aliquot of the reaction mixture was transferred to an NMR tube and heated at 90 °C overnight. The $^{31}P\{^1H\}$ NMR spectrum revealed that two peaks were still present in approximately the same ratio, but that the resonances had now shifted downfield approximately 30 ppm to δ_P = 210.9 and 211.1. There were no observable N–H peaks in the ^1H NMR spectra of **1PCl**-**5PCl** and the IR spectra of the solids lacked N–H vibrations in the range of ν = 3100–3500 cm^{-1}.[44,71] Given these data, the compounds were assigned as the chlorophosphines **1PCl**, **2PCl**, **3PCl**, **4PCl**, and **5PCl** isolated in low to good yields (Table 1). X-ray quality crystals were grown from samples of the bulk powders for **1PCl**-**4PCl** and subsequent X-ray diffraction experiments confirmed the synthesis of the strained, four-membered, cyclic diaminochlorophosphines.

Scheme 2. General method for synthesizing halophosphines with (dianionic)guanidinate ligands.

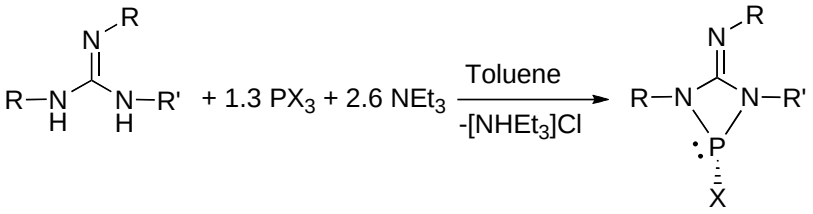

1PCl: R = Mes, R' = Mes, X = Cl
2PCl: R = Dipp, R' = Dipp, X = Cl
3PCl: R = Mes, R' = Dipp, X = Cl
4PCl: R = Dipp, R' = Mes, X = Cl
5PCl: R = Cy, R' = Cy, X = Cl
1PBr: R = Mes, R' = Mes, X = Br

Chart 4. a) Symmetric and b) asymmetric chelating guanidinates for **3PCl**.

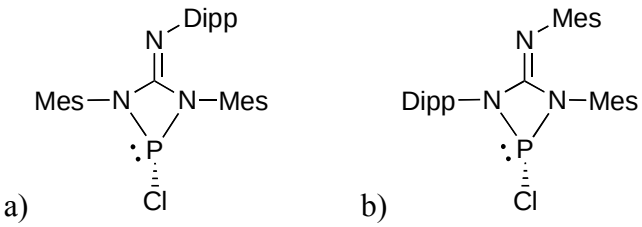

Reactivity. Given the strained nature of these ring systems, we surmised that conversion to the NHP would generate highly reactive cationic phosphorus centres. This transformation was attempted using several metathetical reagents, including a variety of triflate salts (EOTf; E = Me_3Si, Ag, Na, Li; OTf = $[F_3CSO_3]^-$). A stoichiometric amount of Me_3SiOTf was added to CH_2Cl_2 solutions of **1PCl-5PCl** and reaction mixtures were monitored by $^{31}P\{^1H\}$ NMR spectroscopy. At room temperature for **1PCl-4PCl** no change was detected over the course of 7 days, even after the addition of excess amounts of Me_3SiOTf. Identical reaction mixtures were heated to 100 °C in toluene and monitored by $^{31}P\{^1H\}$ NMR spectroscopy, which showed the slow evolution of multiple products, with one peak downfield of the chlorophosphines at $\delta_P = 211$, indicative of the generation of the phosphetidine $Cl_2P_2N_2Mes_2$ (*vide infra*).[68] Analogous results were observed using the sources of metal triflates with **1PCl** over 7 days at

100 °C. Only compound **1PCl** was employed as a model system in subsequent reactivity studies given the simplicity of its solution ^{1}H NMR spectrum. In the case of **5PCl** the addition of Me_3SiOTf results in several products as evidenced by the many signals in the $^{31}P\{^{1}H\}$ NMR spectrum.

Given the difficulty associated with removing chloride from the chlorophosphines, we looked to the bromo- derivatives, as heavier halides generally undergo more facile metathesis.[72] The bromophosphine **1PBr** was synthesized in a similar manner to **1PCl** (Scheme 2, Table 1) and subjected to identical metathesis conditions. Again no reaction or multiple products were observed, none of which corresponded to a downfield chemical shift expected of an NHP in the $^{31}P\{^{1}H\}$ NMR spectra.

Given the puzzling failure of the salt metathesis routes, the Lewis acids $AlCl_3$ and $GaCl_3$ were employed as halide abstracting reagents for **1PCl**. These reactions were also monitored by $^{31}P\{^{1}H\}$ NMR spectroscopy and revealed the formation of single products with upfield chemical shifts ($\Delta\delta_P \approx 10$, Table 1). The volatiles were removed *in vacuo* and the bulk powders were redissolved in $CDCl_3$ to obtain the ^{1}H NMR spectra, which in both cases showed sharp peaks indicating that there was no longer a slow exchange process on the NMR time scale, and furthermore that all symmetry in the molecule was lost. Given the upfield chemical shift in the $^{31}P\{^{1}H\}$ NMR spectra and the lack of symmetry noted in the ^{1}H NMR spectra, it was hypothesized that halide abstraction was not effected, rather a Lewis acid ($AlCl_3$, $GaCl_3$)/Lewis base (N or P) adduct was formed (Scheme 3). Single crystals suitable for X-ray diffraction studies were obtained for the product containing $AlCl_3$ and the solid-state structure confirmed an N→Al adduct of $AlCl_3$ from the exocyclic nitrogen of the guanidinate ligand (**6Al**). Although suitable single crystals for X-ray diffraction studies could not be grown for the $GaCl_3$ adduct (**6Ga**) an identical structure was assigned based on identical ^{1}H NMR spectra and a similar chemical shift in the $^{31}P\{^{1}H\}$ NMR spectrum.

Scheme 3. Lewis acid/Lewis base adduct formation of **6Al** and **6Ga**.

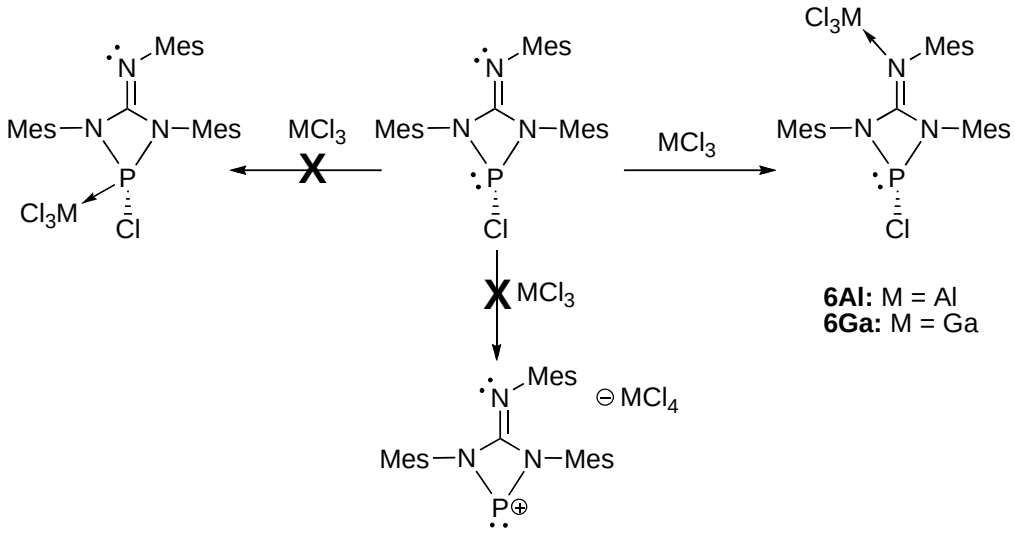

Given the production of **6Al** and **6Ga**, two stoichiometric equivalents of $AlCl_3$ were added to a CH_2Cl_2 solution of **1PCl** at rt, where it was envisaged that the exocyclic nitrogen could be blocked and the second Lewis acid would be free to abstract the chloride ion. After 24 h **6Al** was completely consumed and two phosphorus resonances at δ_P = 165 and 184 were observed. The volatiles were removed *in vacuo* and an orange powder was isolated. A sample of the powder was redissolved in $CDCl_3$ and a ^1H NMR spectrum of the crude material was obtained, which confirmed the presence of multiple products none of which could be isolated separately.

It should be noted that while halide abstraction with these four-membered diaminochlorophosphines appear to be non-trivial, the analogous reaction of those with unsaturated five-membered rings are generally facile.[28,73-77] One major difference between these two species is the additional stabilization gained from the delocalization of a 6π-electron system in the case of the five-membered ring, contrary to the 4π-electrons present in the four-membered ring. While aromaticity is not a necessity for the isolation of NHPs[25,34,35,37,38,67] and has been found to be a weak factor in their stabilization,[75] the lack thereof in our four-membered diaminochlorophosphines may be a contributing factor to the difficulty in halide abstraction.

Given that the isolation of the free NHP was proving to be a difficult feat, an attempt was made to trap the desired phosphenium cation by reaction with a Pt(0) metal centre (Scheme 4), of which

several examples with NHP as ancillary ligands are known.[26,27] The 1:1:1 stoichiometric reaction of **1PCl**, $Pt(PPh_3)_4$, and Me_3SiOTf was monitored by $^{31}P\{^1H\}$ NMR spectroscopy. Combining **1PCl** and $Pt(PPh_3)_4$ resulted in an orange solution which had a change in the $^{31}P\{^1H\}$ NMR spectrum from a singlet to a downfield triplet with Pt satellites for the phosphorus atom of **1PCl** (P_{1PCl}) and an upfield doublet with Pt satellites for coordinated PPh_3 (P_{PPh3}), also free PPh_3 was observed. The splitting pattern was indicative of an AX_2 spin system. The addition of Me_3SiOTf caused a color change to red and an aliquot sampled for $^{31}P\{^1H\}$ NMR spectroscopy showed an upfield shift for the triplet of P_{1PCl}, which had broadened out significantly. The solvent was removed *in vacuo* yielding a red waxy material that became a powder after agitation in hexanes. A sample of the bulk material was used for ^1H NMR spectroscopy (see ESI for spectrum), analysis of the spectrum showed the presence of two products, one of which was identified as free *N,N′*-bis(Mes)carbodiimide. The other product could be isolated in pure form from repeated recrystallizations (x2) from DCM/hexanes at -30 °C. X-ray diffraction studies revealed that the phosphorus containing product was actually the iminophosphine complex of $Pt(PPh_3)_3$, **7**.[78] Although there has been a previous report of cationic iminophosphines acting as ancillary ligands for Ni(0) and Pt(0), no solid-state structures have been obtained.[79]

Scheme 4. Using Pt(0) as a trapping agent.

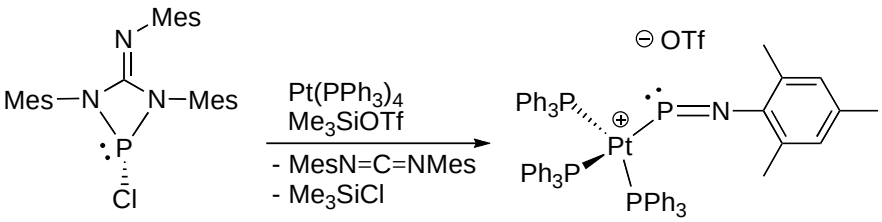

7

Similar to previous work reported by our group,[44] we sought to employ a Lewis base to help support the coordinatively unsaturated phosphenium centre. In this regard, one equivalent of 2,2′-bipyridine (bpy) was added to **1PCl** followed by the addition of Me_3SiOTf (Scheme 5). The color of the solution changed from colorless to yellow. The $^{31}P\{^1H\}$ NMR spectrum showed an upfield shift by $\Delta\delta_P$ = 75 from **1PCl**, as well as a shift corresponding to the starting material, showing no change in intensity between 3 and 24 h. A proton NMR spectrum was collected after removing the solvent *in vacuo* and showed four resonances corresponding to coordinated bpy, and four resonances for free bpy. The product was purified by redissolving in CH_2Cl_2 and adding hexanes to give an oil, which became a powder after drying *in vacuo*. Multinuclear NMR spectroscopy of the purified material showed a single resonance in the $^{31}P\{^1H\}$ NMR spectrum at δ_P = 106 and the loss of peaks corresponding to free bpy in the ^1H NMR spectrum. Single crystals were grown and a solid-state structure was obtained, which confirmed that bpy and a dianionic ligand were coordinated to the phosphorus atom to give the base-stabilized cation, **8**.[78]

Scheme 5. Synthesis of base-stabilized cationic **8**.

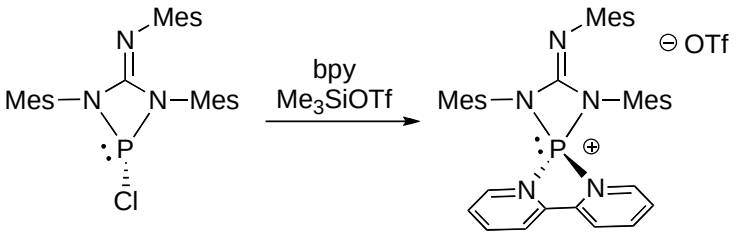

8

Jones *et al*. attempted to reduce a dichlorophosphine supported by a bulky (monoanionic)guanidinate with KC_8, anticipating a diphosphene, however the result was many non-isolable phosphorus containing products.[39] In this context, we investigated the reactivity of **1PCl** with the one-electron reducing agent cobaltocene (Cp_2Co). The 1:1 stoichiometric reaction of **1PCl** and Cp_2Co in THF at room temperature (Scheme 6) produced copious amounts of green precipitate (cobaltocenium chloride; $\delta_H = 5.9$) and monitoring the reaction by $^{31}P\{^1H\}$ NMR spectroscopy revealed the production of a single product at $\delta_P = 59$ ($\Delta\delta_P = 123$). The reaction was complete after 48 h, at which time the green precipitate was removed by centrifugation, the volatiles were removed from the supernatant *in vacuo*, and washing the product with CH_3CN yielded a white powder. The ^1H NMR spectrum of the white powder in $CDCl_3$ at room temperature had four signals in the *aryl* region and five methyl resonances, however if the sample was cooled to -50 °C, six *aryl* and nine methyl signals were observed. X-ray diffraction studies revealed that reductive coupling had occurred, resulting in a dimeric structure with μ-*N*,*N*′ bridging guanidinates for **9**.

Scheme 6. Redox reaction for the synthesis of **9**.

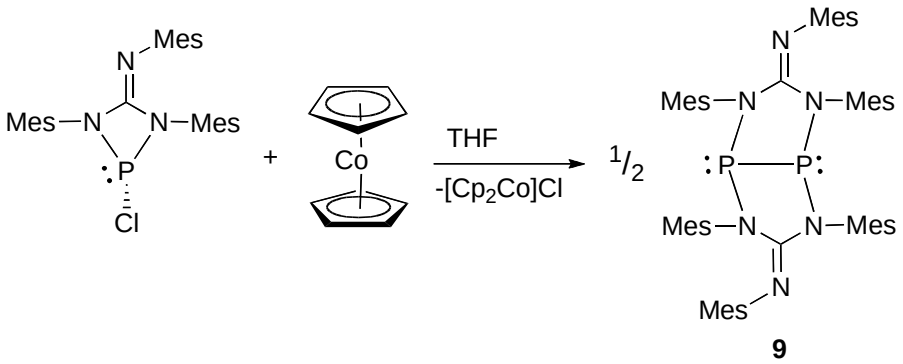

9

The thermal stability of the cyclic four-membered diaminochlorophosphines was investigated given the multiple instances of a peak emerging at $\delta_P \approx 211$ upon heating of these species. This was accomplished by heating a toluene solution of **1PCl** at 90 °C overnight to deduce what had occurred. Resembling the attempted isomerization of **3PCl** and halide abstraction of **1PCl-4PCl**, a 30 ppm downfield chemical shift was noted in the $^{31}P\{^1H\}$ NMR spectrum after 2 days at 90 °C, giving a singlet at $\delta_P = 211$. The product was waxy after the solvent was removed *in vacuo*, but became a white powder after stirring in pentane for 5 min. Decanting the supernatant and drying the powder under reduced pressure yielded pure product as evidenced by ^1H NMR spectroscopy, which showed a drastically simplied spectrum (see ESI). X-ray diffraction studies revealed that the product was indeed the dichlorodiazadiphosphetidine, **10** (see ESI for solid-state structure). The proposed route from **1PCl** to **10** is by elimination of *N,N′*-bis(Mes)carbodiimide resulting in a chloro(2,4,6-trimethylphenylimino)phosphine (MesNPCl), which dimerizes to give a dichlorodiazadiphosphetidine.[80] An analogous dichlorodiazadiarsetidine, $[\{2\text{-}(6\text{-Me})C_5H_3N\}NAsCl]_2$, has been observed by the thermal elimination of Me_3SiCl from $[\{2\text{-}(6\text{-Me})C_5H_3N\}NSiMe_3]AsCl_2$.[42] The thermally induced removal of a carbodiimide fragment from guanidinato molecular species has been comprehensively studied by Barry *et al*. and is a known pathway in their thermal decomposition.[81,82] While **10** was the major product from heating **1PCl**, there was a minor product at $\delta_P = 140$. This species could be isolated from collecting the CH_3CN washes of **10**. Single crystals suitable for X-ray diffraction studies revealed that the minor

product was actually a dinuclear compound featuring a μ-*N*,*N*' bridging guanidinate and a bridging N–Mes (Scheme 7), **11**. Heating a NMR tube charged with **1PCl** in a $CDCl_3$ solution at 90 °C overnight in an oil bath also produces **11** in nearly quantitative yields (92%) according to the $^{31}P\{^1H\}$ NMR spectrum. Possible routes for the ring expansion are proposed as either: (a) ring opening of **1PCl** to dimerize with MesNPCl; or, (b) insertion of *N,N'*-bis(Mes)carbodiimide into a P–N bond of **10** (Scheme 8). To elucidate the likely reaction pathway this reaction was monitored by $^{31}P\{^1H\}$ NMR spectroscopy where a spectrum was collected every hour for 43 h (Figure 1). It was determined that **10** is a short-lived intermediate in the reaction when $CDCl_3$ is used as the solvent (Figure 1b), as the reaction appears to be solvent dependent.[83] Regardless if the route followed proposed mechanism (a) or (b), a 1:1 stoichiometric ratio of **11** and carbodiimide should be observed in the ^1H NMR spectrum of the crude material upon the completion of the reaction, which is indeed the case (Figure 2). Given that the reaction between isolated **10** and *N,N'*-bis(Mes)carbodiimide (Scheme 8b, Eq. 2c) in various stoichiometries (1:1, 1:2, 1:5), solvents and temperatures (toluene (90 °C), xylene (140 °C) and $CDCl_3$ (90 °C)) gave no change in the signals observed within the $^{31}P\{^1H\}$ NMR spectra, it was deduced that the mechanism most likely follows route (a). This is similar to the Lewis acid induced oligomerization observed by Burford *et al*., where an iminophosphine, in equilibrium with the corresponding phosphetidine, is formally inserted into a phosphazane.[84]

Scheme 7. Carbodiimide elimination and ring expansion producing **10** and **11**.

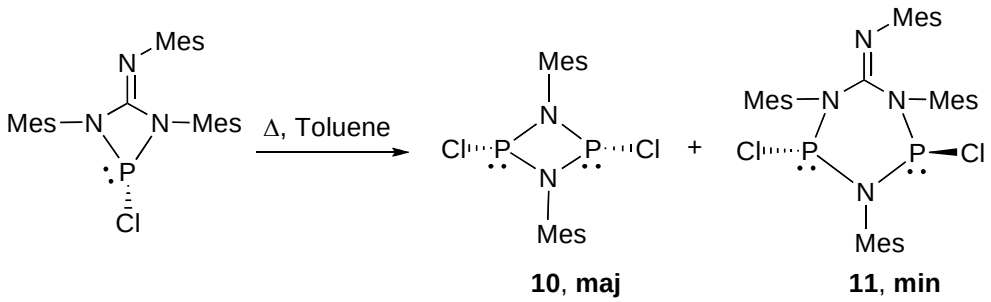

10, **maj** **11**, **min**

Scheme 8. Proposed routes to **11** by a) insertion of MesNPCl or b) insertion of carbodiimide.

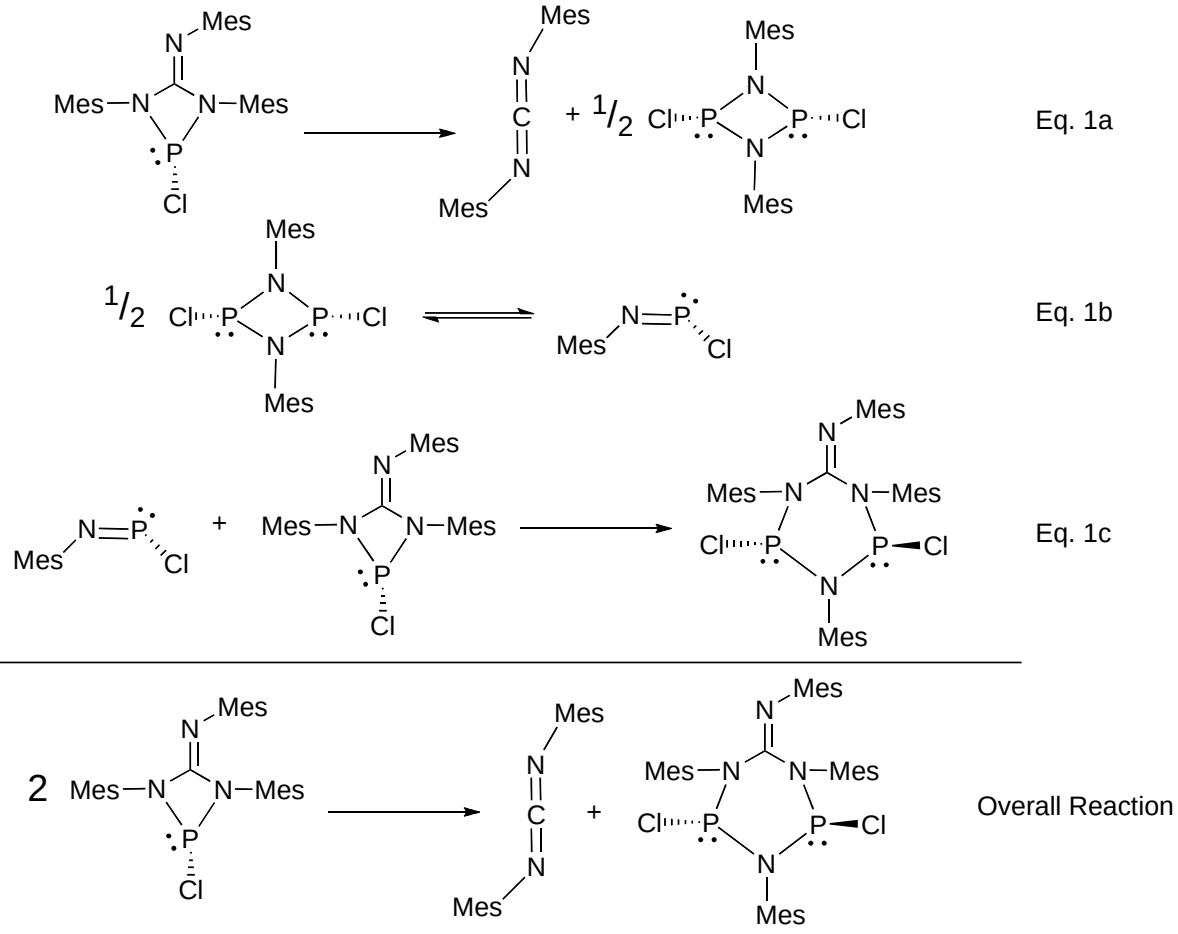

a) Reaction pathway for the insertion of MesNPCl into a P–N bond of **1PCl**. Following the individual steps: (Eq. 1a) the thermal ejection of carbodiimide from **1PCl** to give phosphetidine **10**; (Eq. 1b) monomer/dimer equilibrium of **10** and MesNPCl; and, (Eq. 1c) the insertion of MesNPCl into a P–N bond of **1PCl** to give **11**. Overall, the reaction starts with two equivalents of **1PCl** and ends with equal equivalents of carbodiimide and **11**.

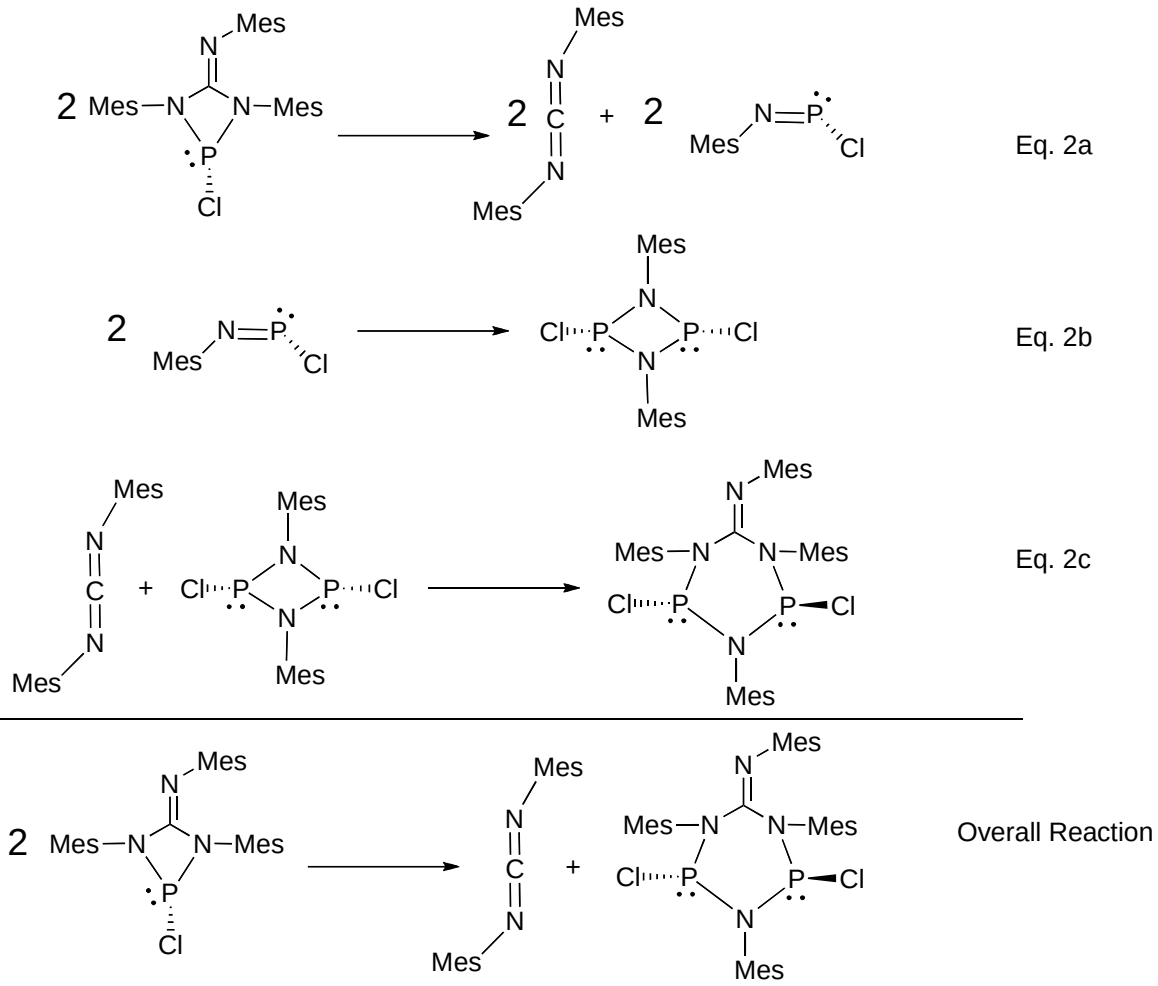

b) Reaction pathway for the insertion of carbodiimide into a P–N bond of **10**. Following the individual steps: (Eq. 2a) the thermal ejection of carbodiimide from **1PCl** to give MesNPCl; (Eq. 2b) dimerization of MesNPCl to **10**; and, (Eq. 2c) the insertion of carbodiimide into a P–N bond of **10** to give **11**. Overall, the reaction starts with two equivalents of **1PCl** and ends with equal equivalents of carbodiimide and **11**.

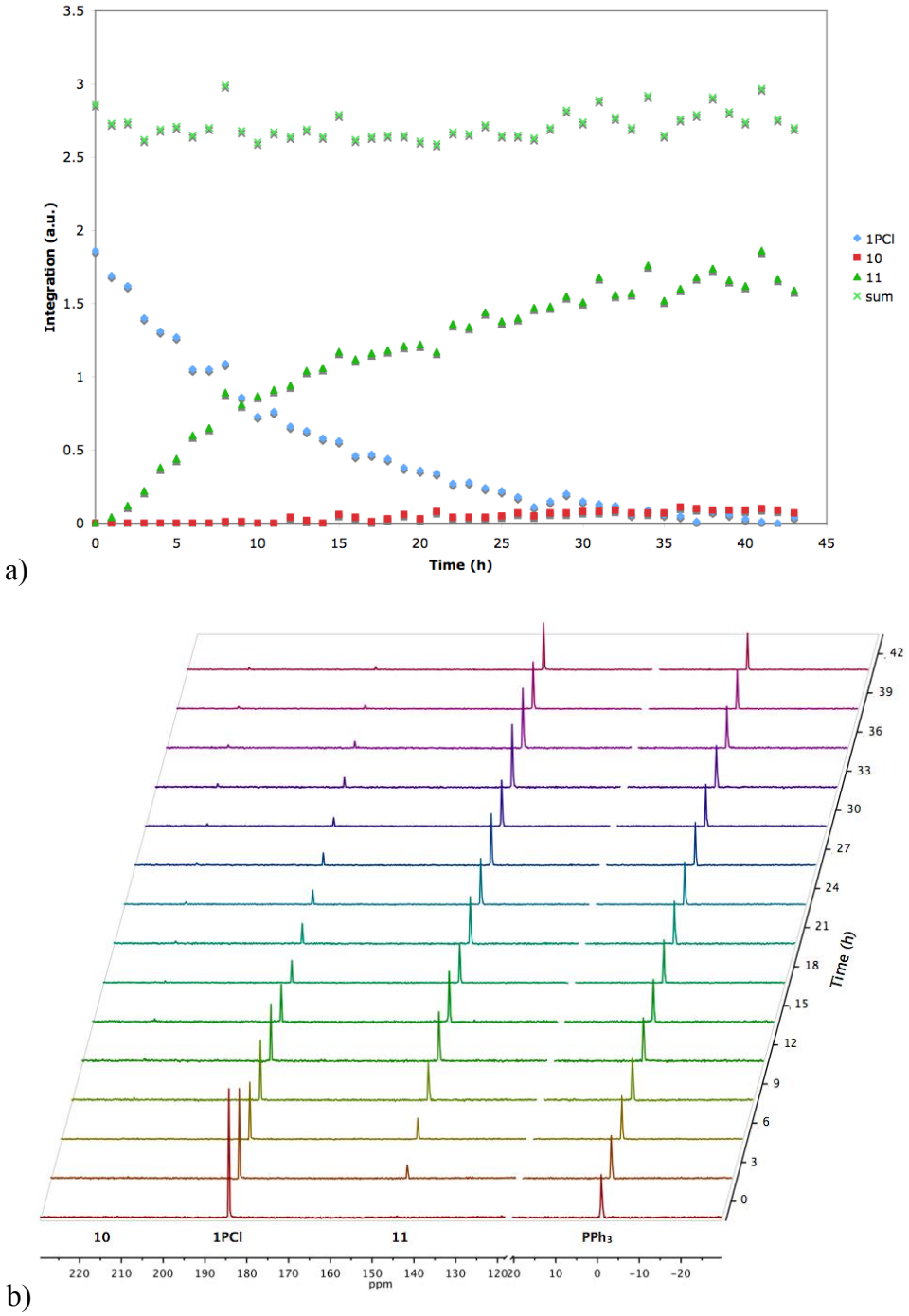

Figure 1. a) Plot of the integration of δ_P **1PCl**, **10**, and **11** relative to normalized PPh_3 and the sum of the integrations as a function of time. b) Stacked plot of $^{31}P\{^1H\}$ NMR spectra for monitoring the production of **11** from **1PCl**.

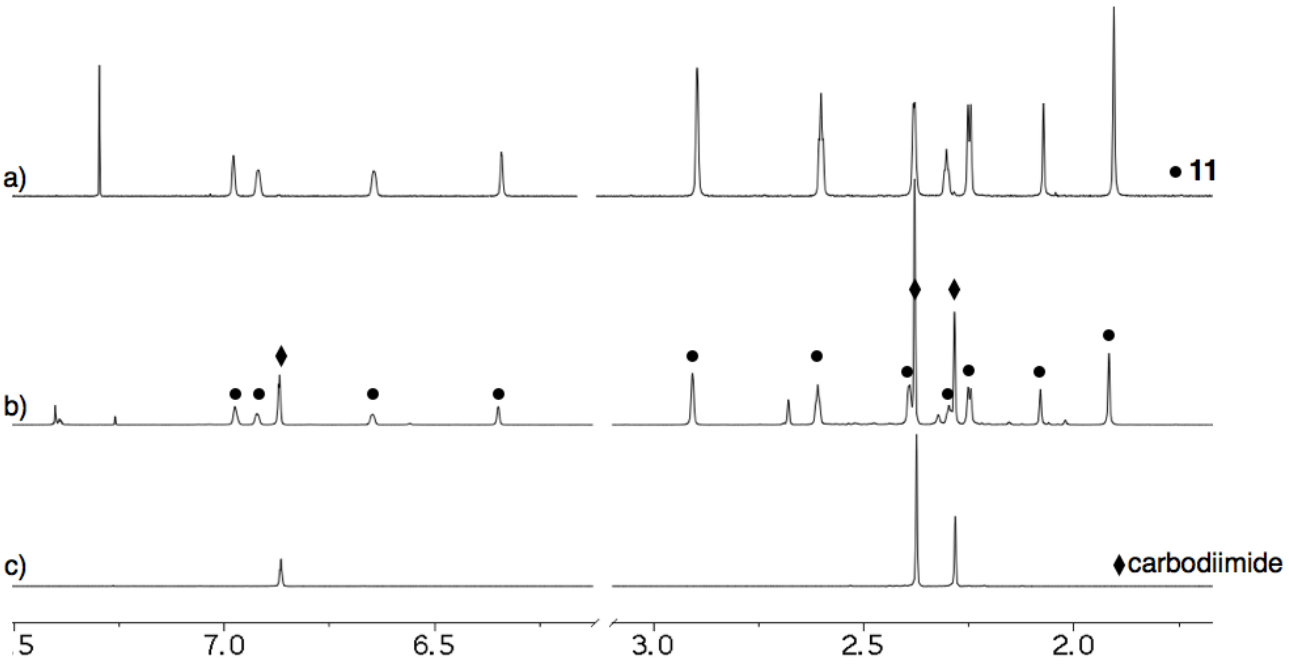

Figure 2. Stack plot of ^{1}H NMR spectra for a) pure **11**, b) crude completed ring expansion, and c) pure *N,N′*-bis(Mes)carbodiimide.

X-Ray Crystallographic Studies. Single crystals suitable for X-ray diffraction studies were grown for compounds **1PCl-4PCl** and **1PBr** by various techniques and solvent combinations (see experimental section for details). The solid-state structures of **1PCl-4PCl** and **1PBr** (Figure 3a-e) are analogous and were all crystallized in the monoclinic $P2_1/c$ space group (Table 2, see Table 1 for summary of important metrical parameters). In all cases, the coordination of the guanidinate ligand to phosphorus is κ^2-*N,N′* chelating, which generates a strained four-membered ring. The N–P–N bond angles range from 75.73(7) – 78.61(7)°, which are on the smaller end of the scale compared to other similar four-membered rings derived from chelating nitrogen-based ligands on phosphorus (*cf.* 70.66 – 120.72°, mean = 87.21°).[85,86] The metrical parameters of the guanidinate ligands further confirmed its dianionic nature in **1PCl-4PCl** and **1PBr**. The C–N_{endo} bond lengths within the ring are consistent with carbon-nitrogen single bonds C(1)–N(1) 1.403(2) – 1.437(2) Å and C(1)–N(2) 1.410(3) – 1.477(2) Å (*cf.* 1.42 (avg) Å)[48] while the C–N_{exo} bond lengths are representative of a carbon-nitrogen double bond C(1)–N(3) 1.249(3) – 1.261(2) Å (*cf.* 1.28 Å).[48] The exocyclic nitrogen N(3) has a stereochemically active lone pair and the *aryl* substituent on N(3) in **3PCl** and **4PCl** resides on the side of the endocyclic

nitrogen bearing the substituent with the least bulk to minimize steric interactions in the case of the heteroleptic guanidinate. The expected trigonal planar geometry is observed about C(1) (Σ_{ang} = 360°) and a pyramidal geometry about P(1) (Σ_{ang} = 280.8 – 287.2°). Short P(1)–Cl(1) bonds are noted for **1PCl-4PCl** with bond lengths ranging from 2.0476(7) – 2.1141(7) Å. This is contrary to the characteristically long P–Cl bonds commonly observed for 6π aromatic cyclic diaminochlorophosphines in the larger five-membered ring, attributed to the hyperconjugation of π(C_2N_2)–σ*(P–Cl) (*e.g.* 2.24 – 2.70 Å).[69,75,87] The P–Cl bond lengths are even shorter than acyclic $(NMe_2)_2PCl$ (2.180(4)).[88] A possible reason for the failed metathesis reactions is the strong phosphorus-halide bond, reflected in the short P–X (X = Cl, Br (2.2936(10) Å, *cf.* 2.43 – 2.95 Å)[28,72,74]) bond distance for **1PCl-4PCl** and **1PBr**.

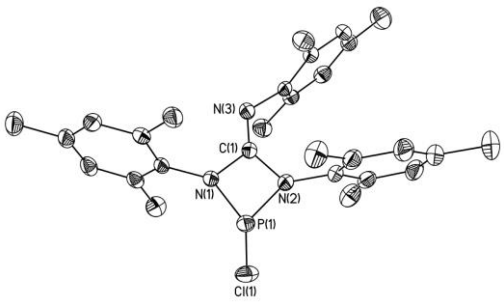

a) **1PCl**

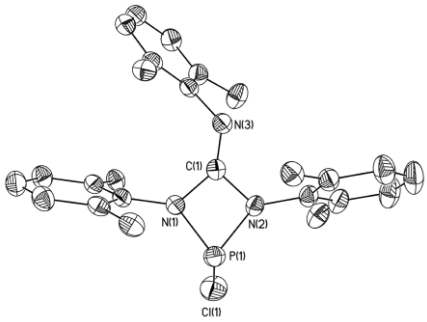

b) **2PCl**

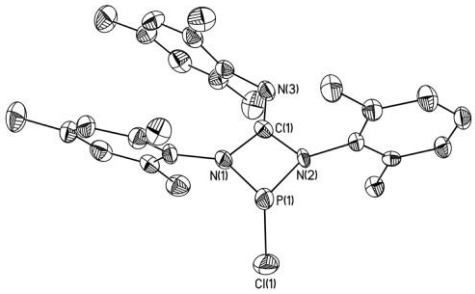

c) **3PCl**

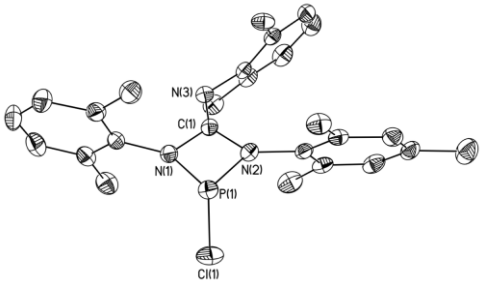

d) **4PCl**

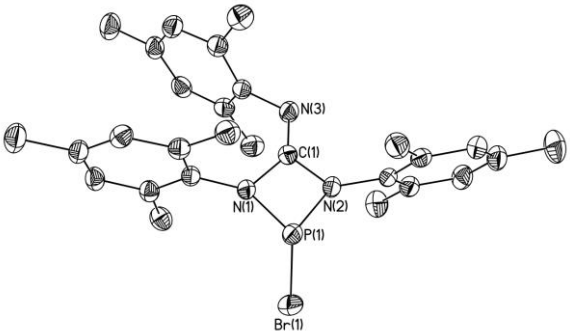

e) **1PBr**

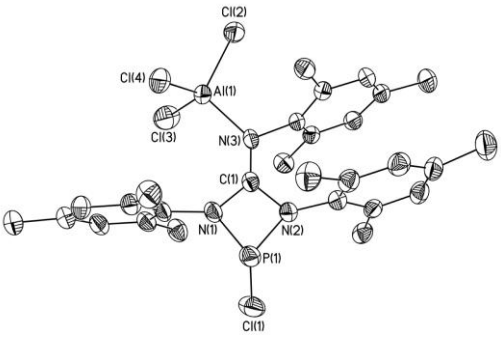

f) **6Al**

Figure 3. Solid-state structures of a) **1PCl**, b) **2PCl**, c) **3PCl**, d) **4PCl**, e) **1PBr**, and f) **6Al**. Ellipsoids are drawn to 50% probability. The methyl groups on the ^{i}Pr substituents, and the hydrogen atoms have been omitted for clarity.

The solid-state structure of **6Al** (Figure 3f, Table 2) confirmed the atom connectivity of N(3) to Al(1) with a bond length of 1.936(3) Å, which is in the typical range found for other $AlCl_3$ adducts.[89,90] Compared to **1PCl**, **6Al** has shortened C(1)–N(1), C(1)–N(2) and P(1)–Cl(1) bond lengths and an

elongated C(1)–N(3) bond (Table 1). The Al–Cl bond lengths have also elongated from 2.068(4) Å in $AlCl_3$ to 2.1132(16) – 2.1304(13) Å in **6Al**.[91] Exocyclic N(3) and endocyclic N(1) have a trigonal planar geometry with the Σ_{ang} = 359.9°, while the sum of the angles about N(2) is 349.8° because of the Mes substituent on N(3) residing above, thus causing a slight pyramidalization to decrease steric interactions.

The most notable structural change of **1PCl** upon reaction with Cp_2Co to form **9** (Figure 4a, Table 2) is the change in the coordination mode of the guanidinate ligand from κ^2-*N*,*N*′ chelating to μ-*N*,*N*′ bridging. The guanidinate ligand **1** retains its dianionic nature in the bridging mode, as indicated by the carbon-nitrogen bond lengths. The P(1)–P(2) bond length is 2.2251(14) Å, which is similar to an analogous structure with μ-*N*,*N*′ bridging ureas (P–P 2.222(2) Å),[92] and consistent with typical P–P single bond lengths (*cf.* 2.21 Å).[86,93] Unlike the planar As_2N_4C bicyclic fragment in a (monoanionic)guanidinate-bridged diarsene,[39] **9** has a puckered arrangement of the two five-membered P_2N_2C rings, where the two planes are 100.4° to each other (Figure 4b). The molecular geometry about the phosphorus atoms is trigonal pyramidal with a stereochemically active lone pair of electrons indicative of an AX_3E electron pair geometry.

The solid-state structure of **11** revealed that a ring expansion of **1PCl** had occurred (Figure 4c). This was most likely the result of monomeric chloro(imino)phosphine inserting into the P–N bond of **1PCl**.[84] Upon ring expansion the coordination of the guanidinate ligand changes from κ^2–*N*,*N*′ chelating to μ-*N*,*N*′ bridging and retains its dianionic charge as indicated by the C(1)–N bond lengths (C(1)–N(1) 1.411(3) Å, C(1)–N(2) 1.416(3) Å, C(1)–N(3) 1.270(3) Å). The P(1)–Cl(1) and P(2)–Cl(2) bond lengths are 2.1228(11) and 2.1290(12) Å, respectively, and significantly longer than **1PCl**. Unlike the phosphetidine **10** the chlorine atoms are in a *trans* conformation and the ring is puckered with a mean deviation from the plane of 0.1425 Å, compared to nearly planar **10** with a mean deviation from the plane of 0.0571 Å. The P–N bonds range from 1.688(2) – 1.704(2) Å, which are shorter than **1PCl**

(1.7081(14) – 1.7235(15) Å) and longer than that of a monomeric chloro(imino)phosphine (P–N 1.495(4) Å for Cl–P=N–Mes*, Mes*=2,4,6-tri-*tert*-butylphenyl).[94]

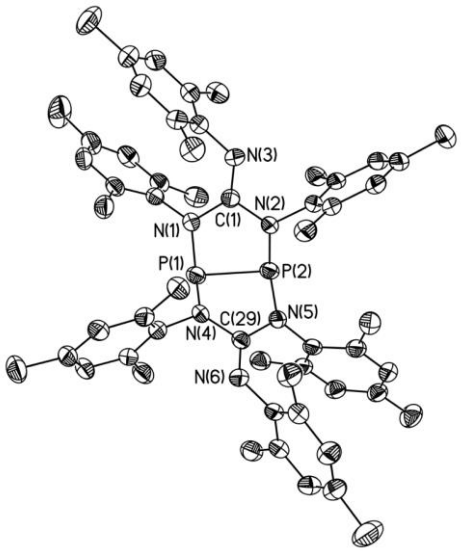

a) **9**

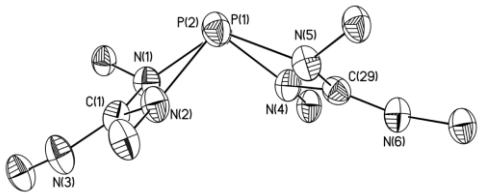

b) **9**

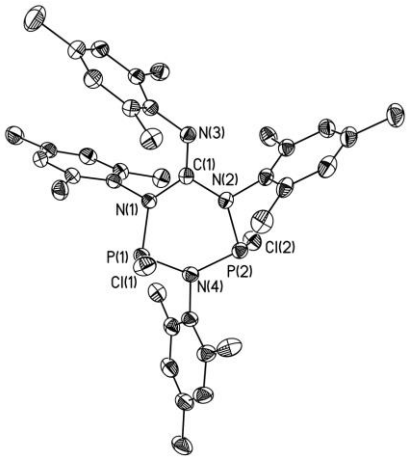

c) **11**

Figure 4. Solid-state structures of a) **9**, b) view of **9** along P-P bond and c) **11**. Ellipsoids are drawn to 50% probability. Hydrogen atoms and solvates have been omitted for clarity. In b) all but the *ipso* carbons removed from the Mes substituents for simplicity. Selected bond lengths (Å) and angles (°): a) P(1)–N(1) 1.725(3), P(1)–N(4) 1.725(3), P(2)–N(2) 1.729(3), P(2)–N(5) 1.721(3), C(1)–N(1) 1.419(5), C(1)–N(2) 1.409(4), C(1)–N(3) 1.265(5), C(29)–N(4) 1.415(4), C(29)–N(5) 1.424(4), C(29)–N(6)

1.266(4), P(1)–P(2) 2.2251(14), N(1)–P(1)–N(4) 108.28(15), N(2)–P(2)–N(5) 108.67(15), N(1)–C(1)–N(2) 111.7(3), N(4)–C(29)–N(5) 110.9(3); and, b) P(1)–Cl(1) 2.1228(11), P(2)–Cl(2) 2.1290(12), P(1)–N(1) 1.696(2), P(1)–N(4) 1.688(2), P(2)–N(2) 1.701(2), P(2)–N(4) 1.704(2), C(1)–N(1) 1.411(3), C(1)–N(2) 1.416(3), C(1)–N(3) 1.270(3), N(1)–P(1)–N(4) 101.36(10), N(2)–P(2)–N(4) 100.52(10), N(1)–C(1)–N(2) 114.7(2).

Table 1. Isolated yields (%) and $^{31}P\{^{1}H\}$ NMR spectroscopy chemical shifts (ppm, $CDCl_3$ solution) for **1PCl-5PCl**, **1PBr**, **6Al**, **6Ga**, and **7-11** and selected bond lengths (Å) and bond angles (°) for **1PCl-4PCl**, **1PBr**, **6Al**.

Compound	**1PCl**	**2PCl**	**3PCl**	**4PCl**	**5PCl**	**1PBr**	**6Al**	**6Ga**	**7**	**8**	**9**	**10**	**11**
Yield	69	72	35	61	31	70	53	66	56	72	61	34	33
δ_P	181	180	181	179	182	200	171	173	147(t), 23 (d)	106	59	211	140
P(1)–N(1)	1.7081(14)	1.716(2)	1.717(5)	1.7592(15)	–	1.722(2)	1.742(3)	–					
P(1)–N(2)	1.7235(15)	1.707(2)	1.690(4)	1.7193(15)	–	1.711(2)	1.743(3)	–					
C(1)–N(1)	1.403(2)	1.427(3)	1.418(7)	1.437(2)	–	1.427(3)	1.375(4)	–					
C(1)–N(2)	1.420(2)	1.410(3)	1.433(7)	1.477(2)	–	1.411(3)	1.398(4)	–					
C(1)–N(3)	1.252(2)	1.249(3)	1.256(7)	1.261(2)	–	1.255(4)	1.304(4)	–					
P(1)–X(1)	2.1141(7)	2.0936(10)	2.095(3)	2.0476(7)	–	2.2936(10)	2.0603(15)	–					
N(1)–P(1)–N(2)	75.73(7)	75.88(9)	76.1(2)	78.61(7)	–	75.97(11)	74.24(12)	–					

Table 2. X-ray details for **1PCl-4PCl**, **1PBr**, **6Al**, and **9**, **11** .

Compound	**1PCl**	**2PCl**	**3PCl**	**4PCl**	**1PBr**	**6Al**	**9**	**11**
empirical formula	$C_{28}H_{33}ClN_3P$	$C_{37}H_{51}ClN_3P$	$C_{31}H_{39}ClN_3P$	$C_{34}H_{45}ClN_3P$	$C_{28}H_{33}BrN_3P$	$C_{28}H_{33}AlCl_4N_3P$	$C_{56}H_{66}N_6P$	$C_{29}H_{94}Cl_6N_{10}P_4$
FW (g/mol)	477.99	604.23	520.07	562.15	522.45	611.32	885.09	1520.22
crystal system	Monoclinic	Monoclinic	Monoclinic	Monoclinic	Monoclinic	Monoclinic	Monoclinic	Triclinic
space group	$P2_1/c$	$P2_1/c$	$P2_1/c$	$P2_1/c$	$P2_1/c$	$P2_1/c$	$P2_1/c$	P-1
a (Å)	8.6540(5)	15.829(3)	20.468(2)	10.744(2)	8.6103(17)	14.544(3)	15.278(3)	11.562(2)
b (Å)	26.8867(14)	11.199(2)	9.2821(10)	15.331(3)	14.299(3)	13.657(3)	21.301(4)	13.418(3)
c (Å)	12.6400(6)	24.175(8)	15.5195(18)	22.699(6)	21.572(4)	17.327(7)	21.126(7)	14.712(3)
α (deg)	90	90	90	90	90	90	90	65.35(3)
β (deg)	115.843(3)	125.42(2)	92.061(4)	118.03(2)	91.13(3)	119.39(2)	133.195(17)	78.17(3)
γ (deg)	90	90	90	90	90	90	90	88.20(3)
V (Å^3)	2646.9(2)	3492.3(15)	2946.6(6)	3300.3(12)	2655.4(9)	2998.7(15)	5012(2)	2026.6(7)
Z	4	4	4	4	4	4	4	1
D_c (mg m^{-3})	1.199	1.149	1.172	1.131	1.307	1.354	1.173	1.246
R_{int}	0.0787	0.0578	0.0827	0.0756	0.0305	0.0534	0.0609	0.1067
$R1[I>2\sigma I]^a$	0.0422	0.0550	0.0894	0.0371	0.0533	0.0557	0.0788	0.0606
$wR2(F^2)^a$	0.1035	0.1687	0.2347	0.1026	0.1424	0.1887	0.2300	0.1461
GOF (S)^a	1.016	1.069	1.126	1.029	1.056	1.083	1.105	1.010

[a] $R1(F[I > 2(I)]) = \sum\| |F_o| - |F_c| \| / \sum |F_o|$; $wR2(F^2$ [all data]) = $[w(F_o^2 - F_c^2)^2]^{1/2}$; S(all data) = $[w(F_o^2 - F_c^2)^2/(n - p)]^{1/2}$ (n = no. of data; p = no. of parameters varied; $w = 1/[\sigma^2(F_o^2) + (aP)^2 + bP]$ where $P = (F_o^2 + 2F_c^2)/3$ and a and b are constants suggested by the refinement program.

Computational Studies. To shed light on the resistance of compounds **1PCl-5PCl** and **1PBr** to halide abstraction, the electronic structures of chlorophosphines **5PCl** and **12PCl-15PCl** (Chart 5) were analyzed using density functional theory (DFT) by determining their charge distributions, orbital structures and relative P–Cl bond energies. For comparison, similar calculations were also performed for chlorophosphines incorporated in four- (P–N–Si–N) and five-membered (P–N–C=C–N) rings **16PCl-19PCl**, which are known to undergo facile metathesis.

Chart 5. Compounds studied computationally.

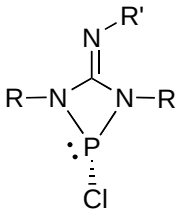

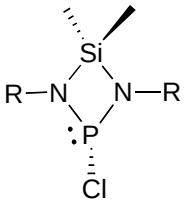

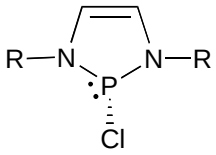

5PCl: R = Cy, R' = Cy
12PCl: R = Ph, R' = Ph
13PCl: R = Ph, R' = ^{t}Bu
14PCl: R = ^{t}Bu, R' = Ph
15PCl: R = ^{t}Bu, R' = ^{t}Bu

16PCl: R = Ph
17PCl: R = ^{t}Bu

18PCl: R = Ph
19PCl: R = ^{t}Bu

Table 3 lists the atomic partial charges for the studied chlorophosphines as obtained from the natural population analysis (NPA) of their Kohn-Sham electron densities.[59] It is necessary to stress that the absolute values of the calculated charges have no physical meaning and it is only their relative magnitudes which yield useful information about structure-induced changes in the electron distribution. The atomic partial charges of phosphorus and carbon in **5PCl** and **12PCl-15PCl** display only small variations, which is in contrast to those calculated for nitrogen and chlorine. These both show a more distinct dependence on the electron withdrawing/donating nature of *N*-substituents, most notably the all-Ph derivative **12PCl** has the least charge concentrated on the electronegative elements within the molecular framework, thereby yielding the least polar P–Cl bond. In contrast, the *N*-alkyl substituted variants **5PCl**, **14PCl** and **15PCl** display a less uniform charge distribution and consequently a more

ionic $P^{\delta+}$–$Cl^{\delta-}$ interaction. These results pinpoint *N*-alkyl derivatives of the target chlorophosphines as the most favorable candidates for halide abstraction. The increased reactivity of the cyclohexyl derivative **5PCl** towards Me_3SiOTf was also observed experimentally (*vide supra*).

A comparison of charge distributions calculated for **5PCl** and **12PCl-15PCl** with those of compounds for which halide abstraction is reported to take place reveals, as expected, that the P–Cl interaction is significantly more ionic in the latter systems. The currently characterized chlorophosphines **16PCl-19PCl** display equal and roughly 0.10 units greater charge separation within the P–Cl bond as compared to the identically *N*-substituted species with a P–N–C–N backbone (see Table 3). Consequently, chlorophosphines with a P–N–C–N backbone appear, by their nature, to be resilient to salt metathesis. To analyze the origin of this phenomenon in detail, we turned our attention to the frontier orbital structure of the corresponding NHPs.

Table 3. Atomic partial charges (δ) as obtained from the natural population analysis of the studied chlorophosphines.

	P	Cl	N	C / Si	Δδ(P–Cl)[b]
5PCl	1.15	-0.36	-0.71[a]	0.59	1.51
12PCl	1.16	-0.32	-0.68[a]	0.60	1.48
13PCl	1.16	-0.33	-0.71[a]	0.59	1.49
14PCl	1.18	-0.37	-0.73[a]	0.61	1.56
15PCl	1.17	-0.38	-0.74[a]	0.61	1.55
16PCl	1.19	-0.38	-1.09	1.98	1.57
17PCl	1.23	-0.45	-1.17	2.02	1.68
18PCl	1.17	-0.42	-0.68	-0.08	1.58
19PCl	1.20	-0.53	-0.71	-0.09	1.72

[a] Average values. [b] Absolute charge difference.

Figure 5 shows the lowest unoccupied molecular (Kohn-Sham) orbitals (LUMOs) and orbital energies of NHPs with different backbones but identical *N*-substituents. This orbital is of particular interest in the study of the nature of bonding in equivalent chlorophosphines as it interacts directly with an electron pair from the halide anion to form the P–Cl bond. Although the overall morphology of the orbitals in Figure 5 is rather similar, a π-type molecular orbital (MO) with a major contribution from the p_z atomic orbital (AO) of phosphorus and a smaller admixture of AOs from the two flanking nitrogen nuclei, their orbital energies are vastly different with the LUMO of our target cations residing by far the lowest. Frontier MO theory based arguments predict that NHPs based on the P–N–C–N backbone should be the best electron acceptors in the series and form the most covalent P–X bonds. The observed differences in the charge distributions of the investigated halophosphines can therefore be correlated with the differing orbital characteristics of the corresponding NHPs. This holds not only for systems shown in Figure 5 but also for other chlorophosphines examined in the current work (see ESI). In addition, we note that the morphology of the LUMO is consistent with the possibility to affect the details of the P–Cl interaction by changing the exocyclic substituents from σ- (alkyl) to π-type (aryl).

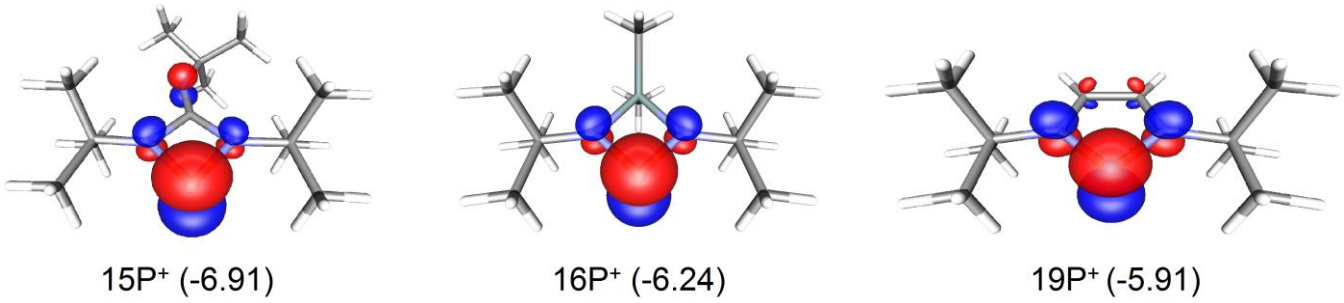

Figure 5. Lowest unoccupied molecular orbitals of the studied *N*-heterocyclic phosphines and their orbital energies (eV, in parenthesis).

Given that our target cations appear to be much better electron acceptors than other known NHPs, the details of the P–X interaction in the corresponding halophosphines should be inferable not only from atomic partial charges but also from calculated bond strengths. We examined the nature of

the P–Cl bond in compounds **5PCl** and **12PCl-15PCl** with the help of energy decomposition analysis (EDA) which partitions the bonding interaction between a cationic NHP and a chloride anion into physically meaningful components (see Table 4).[60] It should be noted here that the instantaneous interaction energy (E_{int}) given by the EDA is not (the negative of) bond dissociation energy, which takes into account the energy gained from relaxation of the fragment geometries upon bond breaking. However, when comparing bonding trends across multiple similar systems, the snapshot-type picture given by the EDA procedure is sufficient.

Table 4. Results from energy decomposition analyses of P–Cl bonding in the studied chlorophosphines.[a]

	E_{Pauli}	E_{elstat}[b]	E_{orb}[b]	E_{int}
5PCl	947	-875 (57%)	-651 (43%)	-580
12PCl	1065	-941 (56%)	-754 (44%)	-630
13PCl	1021	-924 (56%)	-717 (44%)	-621
14PCl	909	-883 (58%)	-628 (42%)	-602
15PCl	910	-870 (58%)	-619 (42%)	-579
16PCl	654	-726 (64%)	-402 (36%)	-475
17PCl	869	-827 (60%)	-551 (40%)	-509
18PCl	774	-801 (62%)	-511 (38%)	-539
19PCl	932	-873 (58%)	-639 (42%)	-580

[a] Energies are reported in kJ mol^{-1}. [b] Percentage of total attractive interactions given in parenthesis

Table 4 lists the calculated EDA interaction energies along with their division into individual contributions from Pauli repulsion (E_{Pauli}) and electrostatic (E_{elstat}) and orbital interactions (E_{orb}). The trend in E_{int} values confirms that the P–Cl bond is markedly stronger in all chlorophosphines with a P–N–C–N backbone as compared to systems previously reported to undergo salt metathesis. The only exception are the fully alkyl substituted **5PCl** and **15PCl** whose interaction energy equals that of **19PCl**.

This is in accord with experimental observations, which demonstrated the increased reactivity of **5PCl** over other halophosphines studied in the present work. Changes in the percentage of E_{orb} from the total attractive interactions (E_{orb} + E_{elstat}) show that as the P–Cl interaction weakens it also becomes more electrostatic in nature. These results are fully in accord with the picture gleaned from the calculated charge distributions and LUMO energies. A correlation analysis on the calculated P–Cl charge difference (Table 3) and the percentage of covalent (orbital-type) character in the P–Cl bond (Table 4) yields a linear relationship with a correlation coefficient $R^2 = 0.93$ (Figure 6a). An equally good linear regression (Figure 6b) is obtained if the LUMO energies of NHPs (see ESI) are plotted against the EDA interaction energies (Table 4).

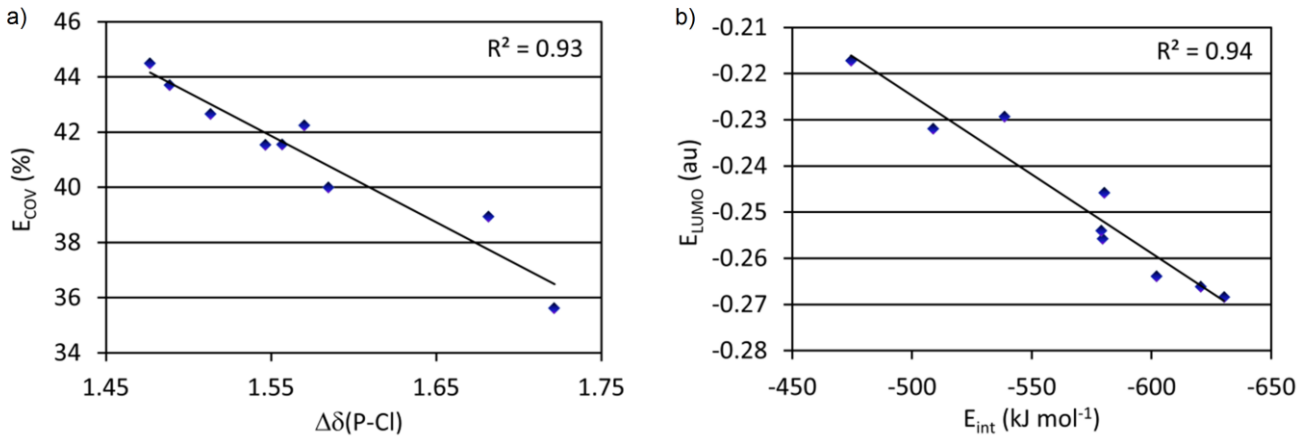

Figure 6. Correlation between a) the covalent contribution and the charge difference in the P–Cl bond of the studied chlorophosphines, and b) correlation between the LUMO energies of the studied NHPs and the EDA P–Cl interaction energies of the studied chlorophosphines.

Investigation of the unoccupied orbitals of the studied chlorophosphines offers a rationale for the role of bpy in capturing the targeted NHP as a base-stabilized cation. As shown in Figure 7 for **12PCl**, both of its two lowest unoccupied orbitals have suitable morphologies to accept electron density from a coordinating Lewis base. A geometry optimization for **12PCl** with bpy was ran and led to the formation

of an adduct with a slightly (0.05 Å) longer P–Cl bond as compared to **12PCl**. This is consistent with the antibonding nature of the orbitals in Figure 7, which in turn implies a weakened P–Cl interaction in the adduct. Consequently, an EDA calculation conducted for the bpy complex of **12PCl** yields a P–Cl interaction energy of –482 kJ mol^{-1} which is significantly less than that obtained for free **12PCl** and similar to that found for chlorophosphines with either P–N–Si–N or P–N–C=C–N backbones (Table 4).

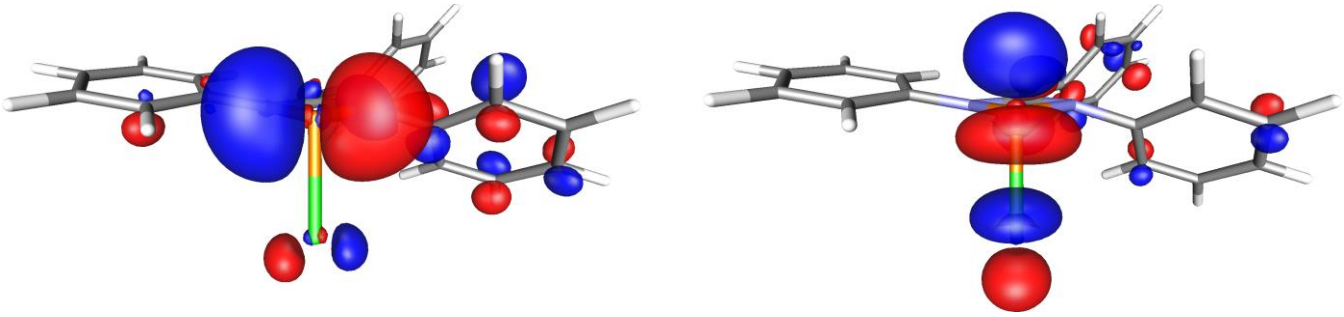

Figure 7. Two of the lowest unoccupied molecular orbitals of **12PCl**.

The collective results from computational investigations enable us to conclude that the exceptionally good electron acceptor properties of the target NHP cations render the corresponding halophosphines reluctant to halide abstraction, unless there is additional stabilization from a Lewis base. The P–X bonds are not only stronger but also more covalent than in analogous systems known to undergo salt metathesis. Consequently, triflate-based reagents show no or only limited reactivity with **1PCl-5PCl**, most likely simply due to increased energy required to break the P–Cl bond.

Conclusion

In summary, **1PCl-4PCl** and **1PBr** represent the first examples of *N*-heterocyclic chlorophosphines supported by (dianionic)guanidinate ligands. The experimentally observed reluctancy to form the corresponding *N*-heterocyclic phosphenium cations was rationalized by computational studies. Analysis of the charge distributions, orbital structures and relative P–Cl bond energies of the computationally studied compounds give corroborating evidence of the strong P–X bond and strong

Lewis acidity of the cationic species. Reactivity studies of **1PCl** demonstrate the high degree of strain induced by the four-membered ring, which leads to chemically and thermally induced carbodiimide elimination, as well as a novel ring expansion by insertion of chloro(imino)phosphine into a P–N bond of **1PCl**. These results demonstrate the electronic nature and alluring reactivity of diaminochlorophosphines restricted in a four-membered ring.

Acknowledgments

The authors gratefully acknowledge the Natural Sciences and Engineering Research Council of Canada (NSERC), the Canada Foundation for Innovation, the Ontario Ministry of Research and Innovation Early Researcher Award (OMRI-ERA), *The* University *of* Western Ontario, the Academy of Finland, the Technology Industries of Finland Centennial Foundation and the University of Jyväskylä for financial support. We also thank CSC – the IT Center for Science in Espoo, Finland for their support in providing computational resources. Dr. C. D. Martin and J. T. Price are also thanked for collection of X-ray diffraction data.

Supporting Information Available. CIF files for **3**, **1PCl-4PCl**, **1PBr**, **6Al**, **9**, **10**, and **11**, solid-state structures of **3**, **4**, **7**, **8**, and **10**, selected ^{1}H NMR spectra, optimized structures and LUMO energies of computationally investigated compounds. This material is available free of charge via the Internet at http://pubs.acs.org.

References and Notes

(1) Spikes, G. H.; Fettinger, J. C.; Power, P. P. *J. Am. Chem. Soc.* **2005**, *127*, 12232.
(2) Peng, Y.; Brynda, M.; Ellis, B. D.; Fettinger, J. C.; Rivard, E.; Power, P. P. *Chem. Commun.* **2008**, 6042.
(3) Li, J.; Schenk, C.; Goedecke, C.; Frenking, G.; Jones, C. *J. Am. Chem. Soc.* **2011**, *133*, 18622.
(4) Power, P. P. *Acc. Chem. Res.* **2011**, *44*, 627.

(5) Peng, Y.; Guo, J.-D.; Ellis, B. D.; Zhu, Z.; Fettinger, J. C.; Nagase, S.; Power, P. P. *J. Am. Chem. Soc.* **2009**, *131*, 16272.
(6) Peng, Y.; Ellis, B. D.; Wang, X.; Power, P. P. *J. Am. Chem. Soc.* **2008**, *130*, 12268.
(7) Zhu, Z.; Wang, X.; Peng, Y.; Lei, H.; Fettinger, J. C.; Rivard, E.; Power, P. P. *Angew. Chem. Int. Ed.* **2009**, *48*, 2031.
(8) Khan, S.; Michel, R.; Dieterich, J. M.; Mata, R. A.; Roesky, H. W.; Demers, J.-P.; Lange, A.; Stalke, D. *J. Am. Chem. Soc.* **2011**, *133*, 17889.
(9) Welch, G. C.; Juan, R. R. S.; Masuda, J. D.; Stephan, D. W. *Science* **2006**, *314*, 1124.
(10) Stephan, D. W.; Erker, G. *Angew. Chem. Int. Ed.* **2010**, *49*, 46.
(11) Dureen, M. A.; Lough, A.; Gilbert, T. M.; Stephan, D. W. *Chem. Commun.* **2008**, 4303.
(12) Mömming, C. M.; Otten, E.; Kehr, G.; Fröhlich, R.; Grimme, S.; Stephan, D. W.; Erker, G. *Angew. Chem. Int. Ed.* **2009**, *48*, 6643.
(13) Ménard, G.; Stephan, D. W. *J. Am. Chem. Soc.* **2010**, *132*, 1796.
(14) Chase, P. A.; Welch, G. C.; Jurca, T.; Stephan, D. W. *Angew. Chem. Int. Ed.* **2007**, *46*, 8050.
(15) Chase, P. A.; Jurca, T.; Stephan, D. W. *Chem. Commun.* **2008**, 1701.
(16) Spies, P.; Schwendemann, S.; Lange, S.; Kehr, G.; Fröhlich, R.; Erker, G. *Angew. Chem. Int. Ed.* **2008**, *47*, 7543.
(17) Sumerin, V.; Schulz, F.; Atsumi, M.; Wang, C.; Nieger, M.; Leskelä, M.; Repo, T.; Pyykkö, P.; Rieger, B. *J. Am. Chem. Soc.* **2008**, *130*, 14117.
(18) Wang, H.; Fröhlich, R.; Kehr, G.; Erker, G. *Chem. Commun.* **2008**, 5966.
(19) Jana, A.; Schulzke, C.; Roesky, H. W. *J. Am. Chem. Soc.* **2009**, *131*, 4600.
(20) Präsang, C.; Stoelzel, M.; Inoue, S.; A]Meltzer, A.; Driess, M. *Angew. Chem. Int. Ed.* **2010**, *49*, 10002.
(21) Payrastre, C.; Madaule, Y.; Wolf, J. G. *Heteroat. Chem* **1992**, *3*, 157.
(22) Burford, N.; Cameron, T. S.; Ragogna, P. J. *J. Am. Chem. Soc.* **2001**, *123*, 7947.
(23) Burford, N.; Ragogna, P. J. *J. Chem. Soc., Dalton Trans.* **2002**, 4307.
(24) Cowley, A. H.; Kemp, R. A. *Chem. Rev.* **1985**, *85*, 367.
(25) Abrams, M. B.; Scott, B. L.; Baker, R. T. *Organometallics* **2000**, *19*, 4944.
(26) Hardman, N. J.; Abrams, M. B.; Pribisko, M. A.; Gilbert, T. M.; Martin, R. L.; Kubas, G. J.; Baker, R. T. *Angew. Chem. Int. Ed.* **2004**, *43*, 1955.
(27) Caputo, C. A.; Jennings, M. C.; Tuononen, H. M.; Jones, N. D. *Organometallics* **2009**, *28*, 990.
(28) Caputo, C. A.; Brazeau, A. L.; Hynes, Z.; Price, J. T.; Tuononen, H. M.; Jones, N. D. *Organometallics* **2009**, *28*, 5261.
(29) Spinney, H. A.; Yap, G. P. A.; Korobkov, I.; DiLabio, G.; Richeson, D. S. *Organometallics* **2006**, *25*, 3541.
(30) Montemayor, R. G.; Sauer, D. T.; Fleming, S. S.; Bennett, D. W.; Thomas, M. G.; Parry, R. W. *J. Am. Chem. Soc.* **1978**, *100*, 2231.
(31) Nakazawa, H.; Yamaguchi, Y.; Mizuta, T.; Miyoshi, K. *Organometallics* **1995**, *14*, 4173.
(32) Burck, S.; Daniels, J.; Gans-Eichler, T.; Gudat, D.; Nättinen, K.; Nieger, M. *Z. Anorg. Allg. Chem.* **2005**, *631*, 1403.
(33) Burford, N.; Dyker, C. A.; Decken, A. *Angew. Chem. Int. Ed.* **2005**, *44*, 2364.
(34) Holthausen, M. H.; Weigand, J. J. *J. Am. Chem. Soc.* **2009**, *131*, 14210.
(35) Holthausen, M. H.; Richter, C.; Hepp, A.; Weigand, J. J. *Chem. Commun.* **2010**, *46*, 6921.
(36) Weigand, J. J.; Feldman, K.-O.; Henne, F. D. *J. Am. Chem. Soc.* **2010**, *132*, 16321.
(37) Scherer, O. J.; Schnabl, G. *Chem. Ber.* **1976**, *109*, 2996.
(38) Niecke, E.; Kröher, R. *Angew. Chem. Int. Ed.* **1976**, *15*, 692.
(39) Green, S. P.; Jones, C.; Jin, G.; Stasch, A. *Inorg. Chem.* **2007**, *46*, 8.
(40) Ergezinger, C.; Weller, F.; Dehnicke, K. *Z. Naturforsch., B: Chem. Sci.* **1988**, *43*, 1119.

(41) Raston, C. L.; Skelton, B. W.; Tolhurst, V.-A.; White, A. H. *Polyhedron* **1998**, *17*, 935.
(42) Raston, C. L.; Skelton, B. W.; Tolhurst, V.-A.; White, A. H. *J. Chem. Soc., Dalton Trans.* **2000**, 1279.
(43) Lyhs, B.; Schulz, S.; Westphal, U.; Bläser, D.; Boese, R.; Bolte, M. *Eur. J. Inorg. Chem.* **2009**, 2247.
(44) Brazeau, A. L.; Nikouline, A. S.; Ragogna, P. J. *Chem. Commun.* **2011**, *47*, 4817.
(45) Bailey, P. J.; Gould, R. O.; Harmer, C. N.; Pace, S.; Steiner, A.; Wright, D. S. *Chem. Commun.* **1997**, 1161.
(46) Findlater, M.; Hill, N. J.; Cowley, A. H. *Dalton Trans.* **2008**, 4419.
(47) Boeré, R. E.; Boeré, R. T.; Masuda, J.; Wolmershäuser, G. *Can. J. Chem.* **2000**, *78*, 1613.
(48) Tin, M. K. T.; Yap, G. P. A.; Richeson, D. S. *Inorg. Chem.* **1998**, *37*, 6728.
(49) Attempts to obtain HRMS for **1PCl-5PCl**, **1PBr** were unsuccessful because the molecule fell apart and only compounds **1**–**5** are observed in the spectrum.
(50) Lower temperature NMR spectroscopy was used in acquiring the 1H and 13C{1H} NMR spectra for compounds **1PCl-5PCl**, **1PBr**, and **9**. At room temperature the resonances were broad due to dynamic processes.
(51) TURBOMOLE V6.3 2011, a development of University of Karlsruhe and Forschungszentrum Karlsruhe GmbH, 1989-2007, TURBOMOLE GmbH, since 2007; available from http://www.turbomole.com.
(52) ADF2010, SCM, Theoretical Chemistry, Vrije Universiteit, Amsterdam, The Netherlands, http://www.scm.com.
(53) Perdew, J. P.; Burke, K.; Ernzerhof, M. *Phys. Rev. Lett.* **1996**, *77*, 3865.
(54) Perdew, J. P.; Burke, K.; Ernzerhof, M. *Phys. Rev. Lett.* **1997**, *78*, 1396.
(55) Perdew, J. P.; Ernzerhof, M.; Burke, K. *J. Chem. Phys.* **1996**, *105*, 9982.
(56) Adamo, C.; Barone, V. *J. Chem. Phys.* **1999**, *10*, 6158.
(57) Weigend, F.; Häser, M.; Patzelt, H.; Ahlrichs, R. *Chem. Phys. Lett.* **1998**, *294*, 143.
(58) Weigend, F.; Ahlrichs, R. *Phys. Chem. Chem. Phys.* **2005**, *7*, 3297.
(59) Reed, A. E.; Weinstock, R. B.; Weinhold, F. *J. Chem. Phys.* **1985**, *83*, 735.
(60) Bickelhaupt, F. M.; Baerends, E. J. In *Rev. Comput. Chem.*; Lipkowitz, K. B., Boyd, D. B., Eds.; Wiley-VCH: New York, 2000; Vol. 15, p 1.
(61) Morokuma, K. *J. Chem. Phys.* **1971**, *55*, 1236.
(62) Kitaura, K.; Morokuma, K. *Int. J. Quantum Chem* **1976**, *10*, 325.
(63) Ziegler, T.; Rauk, A. *Theoret. Chim. Acta* **1977**, *46*, 1.
(64) van Lenthe, E.; Baerends, E. J. *J. Comput. Chem.* **2003**, *24*, 1142.
(65) Laaksonen, L. *J. Mol. Graphics* **1992**, *10*, 33.
(66) Bergman, D. L.; Laaksonen, L.; Laaksonen, A. *J. Mol. Graphics Modell.* **1997**, *15*, 301.
(67) Caputo, C. A.; Price, J. T.; Jennings, M. C.; McDonald, R.; Jones, N. D. *Dalton Trans.* **2008**, 3461.
(68) Burford, N.; Cameron, T. S.; Conroy, K. D.; Ellis, B.; Macdonald, C. L. B.; Ovans, R.; Phillips, A. D.; Ragogna, P. J.; Walsh, D. *Can. J. Chem.* **2002**, *80*, 1404.
(69) Burck, S.; Gudat, D.; Nättinen, K.; Nieger, M.; Niemeyer, M.; Schmid, D. *Eur. J. Inorg. Chem.* **2007**, 5112.
(70) Denk, M. K.; Gupta, S.; Ramachandran, R. *Tetrahedron Lett.* **1996**, *37*, 9025.
(71) Pavia, D. L.; Lampman, G. M.; Kriz, G. S. *Introduction to Spectroscopy*; 2nd ed.; Saunders College Publishing: Orlando, 1996.
(72) Burck, S.; Gudat, D.; Nieger, M.; Benkö, Z.; Nyulászi, L. *Z. Anorg. Allg. Chem.* **2009**, *635*, 245.
(73) Reeske, G.; Cowley, A. H. *Inorg. Chem.* **2007**, *46*, 1426.
(74) Dube, J. W.; Farrar, G. J.; Norton, E. L.; Szekely, K. L. S.; Cooper, B. F. T.; Macdonald, C. L. B. *Organometallics* **2009**, *28*, 4377.
(75) Gudat, D.; Haghverdi, A.; Hupfer, H.; Nieger, M. *Chem. Eur. J.* **2000**, *6*, 3414.

(76) Carmalt, C. J.; Lomeli, V.; McBurnett, B. G.; Cowley, A. H. *Chem. Commun.* **1997**, 2095.

(77) Denk, M. K.; Gupta, S.; Lough, A. J. *Eur. J. Inorg. Chem.* **1999**, 41.

(78) Several solvents and techniques were attempted for the crystallization of **7** and **8**, and while X-ray quality single crystals suitable for diffraction studies were grown and the data collected, a highly disordered anion was present in each, which could not be modelled appropriately. The solid-state structures of the cations, confirming the identity and connectivity are presented in the ESI.

(79) Niecke, E.; Nixon, J. F.; Wenderoth, P.; Passos, B. F. T.; Nieger, M. *J. Chem. Soc., Chem. Commun.* **1993**, 846.

(80) Lehmann, M.; Schulz, A.; Villinger, A. *Struct. Chem.* **2011**, *22*, 35.

(81) Coyle, J. P.; Johnson, P. A.; DiLabio, G. A.; Barry, S. T.; Müller, J. *Inorg. Chem.* **2010**, *49*, 2844.

(82) Ziffle, L. C.; Kenney, A. P.; Barry, S. T.; Müller, J. *Polyhedron* **2008**, *27*, 1832.

(83) It was observed experimentally that **11** was produced in significantly higher yields and shorter time if $CDCl_3$ was used as the solvent compared to toluene. However, no further solvent dependency experiments were conducted.

(84) Burford, N.; Cameron, T. S.; Conroy, K. D.; Ellis, B.; Lumsden, M.; Macdonald, C. L. B.; McDonald, R.; Philips, A. D.; Ragogna, P. J.; Schurko, R. W.; Walsh, D.; Wasylishen, R. E. *J. Am. Chem. Soc.* **2002**, *124*, 14012.

(85) Average of the result of a query in the CSD for N-P-N angle of four-membered rings featuring chelating N-based ligands. Accessed 9 November 2011.

(86) Bruno, I. J.; Cole, J. C.; Edgington, P. R.; Kessler, M.; Macrae, C. F.; McCabe, P.; Pearson, J.; Taylor, R. *Acta Crystallogr., Sect. B: Struct. Sci* **2002**, *58*, 389.

(87) Gudat, D. *Acc. Chem. Res.* **2010**, *43*, 1307.

(88) Zaripov, N. M.; Naumov, V. A.; Tuzova, L. L. *Phosphorus* **1974**, *4*, 179.

(89) Grant, D. F.; Killean, R. C. G.; Lawrence, J. L. *Acta Crystallogr., Sect. B: Struct. Sci* **1969**, *B25*, 377.

(90) Thomas, F.; Bauer, T.; Schulz, S.; Nieger, M. *Z. Anorg. Allg. Chem.* **2003**, *629*, 2018.

(91) Timoshkin, A. Y.; Suvorov, A. V.; Bettinger, H. F.; Schaefer, H. F. *J. Am. Chem. Soc.* **1999**, *121*, 5687.

(92) Roesky, H. W.; Zamankhan, H.; Sheldrick, W. S.; Cowley, A. H.; Mehrotra, S. K. *Inorg. Chem.* **1981**, *20*, 2910.

(93) Mean value observed for P–P single bonds in literature based on a CSD search on 21 November 2011.

(94) Niecke, E.; Nieger, M.; Reichert, F. *Angew. Chem. Int. Ed.* **1988**, *27*, 1715.